A sulfoxide-based isobaric labelling reagent for accurate quantitative mass spectrometry

Michael Stadlmeier[a],+, Jana Bogena[a],+, Miriam Wallner[a],+, Martin Wühr[b] and Thomas Carell[a],*

[a] Center for Integrated Protein Science at the Department of Chemistry, Ludwig-Maximilians-Universität München, Butenandtstr. 5-13, 81377 Munich, Germany

[b] Department of Molecular Biology & the Lewis-Sigler Institute for Integrative Genomics, Princeton University, Princeton, NJ 08544, USA

[+] These authors contributed equally to this work.

* Corresponding author E-Mail: Thomas.Carell@lmu.de

The article was published online 08.01.2018 in Angewandte Chemie International Edition
DOI: 10.1002/anie.201708867 Print: 57(11):2958 - 2962

Abstract: *Modern proteomics requires reagents for exact quantification of peptides in complex mixtures. Peptide labelling is most typically achieved with isobaric tags that consist of a balancer and a reporter part that separate in the gas phase. An ingenious distribution of stable isotopes provides multiple reagents with identical molecular weight but a different mass of the reporter groups, allowing relative quantification of multiple samples in one measurement. Current generation reagents require a high fragmentation energy for cleavage, leading to incomplete fragmentation and hence loss of signal intensity. Here we report a new isobaric labelling reagent, where the balancer and the reporter are linked by a sulfoxide group, which, based on the sulfoxide pyrolysis, leads to easy and asymmetric cleavage at low fragmentation energy. The fragmentation of our new design is significantly improved, yielding more intense complementary ion signals, allowing complementary ion cluster analysis as well.*

After the development of new genome sequencing methods that allow human genomics studies in just a few hours,[1] today, we are witnessing the emergence of novel mass spectrometry methods that enable the investigation of the complete proteomes of cells and tissues.[2-4] The proteome is defined as the collection of all proteins present in a sample and hence proteomes differ dramatically from cell type to cell type and in different tissues.[5] Proteomics data therefore provide fingerprint-type information about cellular situations and potentially existing disease states.[6] To gain deep insight into the proteome of biological systems, it is necessary to obtain quantitative information about the levels of the individual proteins in the different samples. Nowadays, this is performed with mass spectrometry. Since exact quantification of intact proteins is difficult, the proteomes need to be digested (trypsinated) to give the corresponding peptides. For quantification of these peptides, methods such as metabolic labelling,[7-8] label-free quantification[9] or isobaric labelling[10-11] are performed. Since isobaric labelling is able to reveal even small differences in peptide abundances and because many samples can be compared in one measurement, it is one of the most commonly used quantification methods.[12] A typical proteomics experiment illustrating the procedure is shown in Fig. 1A.

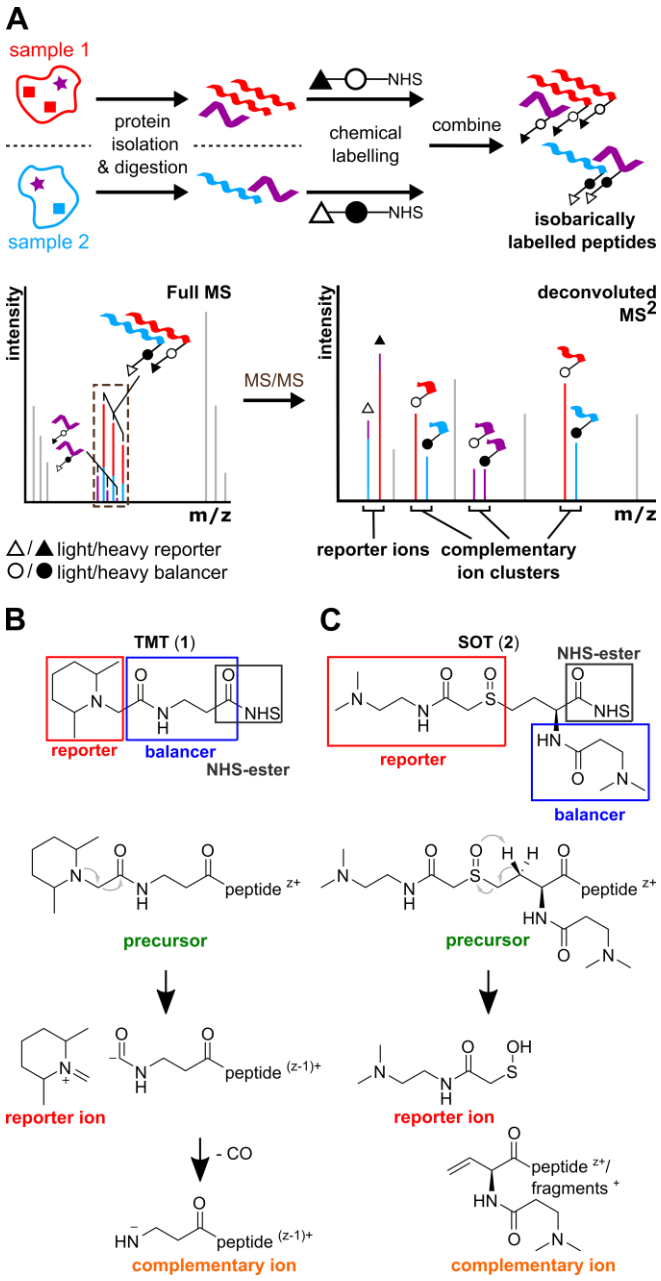

Figure 1. A) Isobaric labelling experiment for quantitative proteomics. The samples are individually labelled with isotopologues of the reagents **1** or **2** and combined for LC-MS² studies. Fragmentation in the gas phase yields reporter and complementary ions for relative quantification. The reporter ion ratio is distorted by co-isolated peptides (purple). The complementary ion clusters can be analysed without such a distortion. B) Currently used TMT (**1**) reagent. Fragmentation introduces a negative charge on the balancer, reducing the overall charge state on the complementary ions. C) SulfOxide Tag (SOT**, 2**) reported in this study with a charge-neutral fragmentation that retains all charges on the complementary ions to facilitate fragmentation.

The proteomes of two samples are isolated, digested and the peptides are reacted with an isobaric labelling reagent such as the Tandem Mass Tag (TMT) reagent **1** (Fig. 1B) or the new labelling reagent **2** (Fig. 1C) reported in this study. The prepared derivatised peptide mixtures are next combined and the mixture is analysed by HPLC-MS[13] or even CE-MS.[14-15] During separation, the same peptides derived from the two samples (blue and red in Fig. 1) will feature the same retention time due to the isobaric character of the labels. They will consequently enter the mass spectrometer at the same time, leading to one indistinguishable m/z-value in the full MS-scan. This allows performing mass spectrometry-based identification by selecting a single precursor m/z for fragmentation (MS²). Cleavage of the isobaric labels provides two now different reporter ions (Δ, Fig 1A), which allows relative quantification. The sensitivity of the methods depends on the cleavage efficiency.

In addition to a reporter ion, a balancer-peptide conjugate, the complementary ion, is also generated from each peptide. Because the attached balancer retains the distinct isotope pattern from the isobaric labelling reagent, the complementary ions allow quantification as well.[16] This even has the advantage that co-eluting peptides (purple), which give reporter ions indistinguishable from the reporter signals of interest, cannot disturb the signal. This problem, known as ratio distortion, often hinders accurate quantification based on reporter ion analysis.[17] Again, sensitivity is determined by cleavage efficiency and this is a drawback of the contemporary reagents.[16]

Here we report the development of a new SulfOxide Tag reagent **2** (SOT, Scheme 1 A) that fragments more easily, which improves quantitation. Importantly, the reagent features two basic *tert*-amino groups, which are protonated in the gas phase. This avoids formation of neutral species

during reagent cleavage and it increases the charge density, which facilitates fragmentation. The SOT reagent **2** design allows the introduction of up to eight heavy stable isotopes into the structure generating reporters with $\Delta m/z = 1$, while keeping isobaricity. This design was chosen to enable mass spectrometric quantification of nine different samples in parallel with one single measurement. The proposed structures of this higher 9-plex reagents are shown in the SI (Supporting Fig. 3).

The synthesis of reagent **2** and of two isobaric isotope derivatives (**2**^{179} and **2**^{180}), which feature different reporter ion molecular weights (179 Da and 180 Da), is shown in Scheme 1B. To our knowledge, the masses of the generated reporter ions do not coincide with immonium- or other frequently observed fragment ions. The synthesis (Supporting Information) starts with the methylester of the homocystine dimer **3**, which is first converted with dimethylamino propionic acid into the bis-amide **4**. Reduction of the disulfide and alkylation of the thiol with benzyl bromoacetate furnishes the key intermediate **5**. Cleavage of the benzylester to **6** and reaction of **6** with 1,1-dimethylethylenediamine gives the bisamide **7**. Saponification of the methylester in **7** to **8**, oxidation of the sulfide to the sulfoxide **9** and conversion of the acid provides reagent **2** as the active ester. To access the isotopologues, we replaced the dimethylamino propionic acid by the similar compound **10** in which one methyl group carries a ^{13}C atom (SI) in a second synthesis. In a third synthesis, we used the ^{13}C-labelled benzyl bromoacetate **11** (SI). This gave the corresponding reagents **2**^{179} and **2**^{180} (Scheme 1A) in similar yields. The synthesis takes roughly one week, and the overall yield is ca. 12%. Storing the reagent in pure form or even in a stock solution (DMSO) is possible at -20 °C for several weeks.

To examine the fragmentation properties of SOT **2**, we digested a *HEK* lysate, containing all translated proteins into the corresponding peptides following a standard protocol (SI). The obtained complex peptide mixture (P) was divided into two portions. While one portion was reacted with reagent **2**^{179} (P-2^{179}) the other was combined with **2**^{180} to give P-2^{180} (pH = 8.5, 150 mM triethylammonium bicarbonate buffer, 1.5 mg **2**^{179} or **2**^{180}, 60 min). We subsequently quenched unreacted reagent **2** with hydroxylamine. Next, the labelled mixtures {P-2^{179}+P-2^{180}} were combined in a 1:1 ratio, and the complex mixture was desalted and concentrated according to reported procedures.[18]

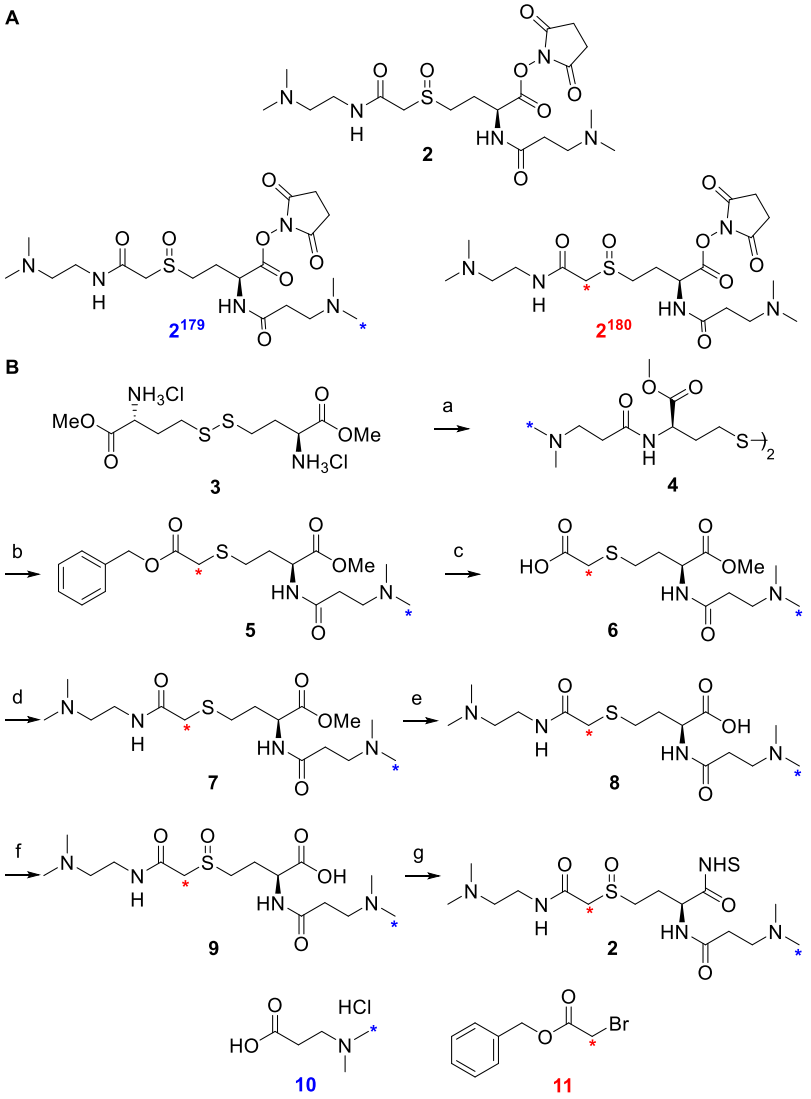

Scheme 1. A) Depiction of the new reagent **2** and of the isotopologues **2**^{179} and **2**^{180}. B) a) 3-(Dimethylamino)propionic acid hydrochloride, NEt_3, HOBt, 60 °C, 2 h, 85%; b) Over two steps i) TCEP*HCl, $NaHCO_3$, H_2O/DMF (4:1), r.t., 10 min; ii) Benzyl bromoacetate, r.t., 2 h, 95%; c) 10% Formic acid in MeOH, 100 wt% Pd black, 40 °C, 2 h, 81%; d) *N*,*N*'-dimethylethane-1,2-diamine, DIPEA, PyBOP, DMF, 40 °C, 1 h, 73%; e) LiOH, MeOH/H_2O (2.5:1), r.t., 1 h, quant.; f) pH = 2, *m*CPBA, H_2O, r.t., 20 min, 75%; g) NHS-TFA, pyridine, DMF, r.t., 2 h, 35%. 179 Da and 180 Da are the molecular weights of the generated reporter ions.

For comparison, we performed the same experiment with the commercially available isotopically labelled TMT reagents **1** (duplex) according to manufacturer's recommendations to obtain the mixture {P-TMT^{126} + P-TMT^{127}}. The peptide mixtures {P-2^{179} + P-2^{180}} and {P-TMT^{126} + P-TMT^{127}} were next measured by nanoHPLC-MS^2 and the data were analysed using the MaxQuant software and a software package developed in-house (Supplementary Figure 1&2).[19] The obtained data are depicted in Fig. 2 and Fig. 3. As an example, Fig. 2A shows the cleavage of the SOT reagent **2** after reaction with the peptide DLPEHAVLK^{2+} (bearing two labels) in direct comparison to the corresponding TMT labelled peptide in the complex mixture. We measured at a normalized fragmentation energy of 28% HCD (*higher-energy collisional dissociation*), which is ideally suited to fragment peptides for their identification. The SOT reagent **2** clearly generates higher intensity reporter ions and in addition, we observe more fragmentation, indicating that the reagent supports peptide fragmentation. Fig. 2B shows an analysis of all peptides identified in the SOT- and TMT-labelled sample and here, we see that in most MS²-spectra, the relative reporter ion intensity for the SOT-sample is as high as 70-100%, which is unprecedented. This enables easy relative quantification by determining reporter ion ratios with available software packages. In comparison, TMT-labelled peptides produce reporter ions of lower relative intensity at this HCD-energy. Fig. 2C shows the charge states of the intact labelled peptides before fragmentation (precursors). In agreement with our design, we see that the SOT reagent **2** generates labelled peptides with much higher charge states. Importantly, more than 65% of the labelled peptides have charge states equal to or above +3. This high charge density facilitates the subsequent fragmentation, which results in the formation of more complementary ions.

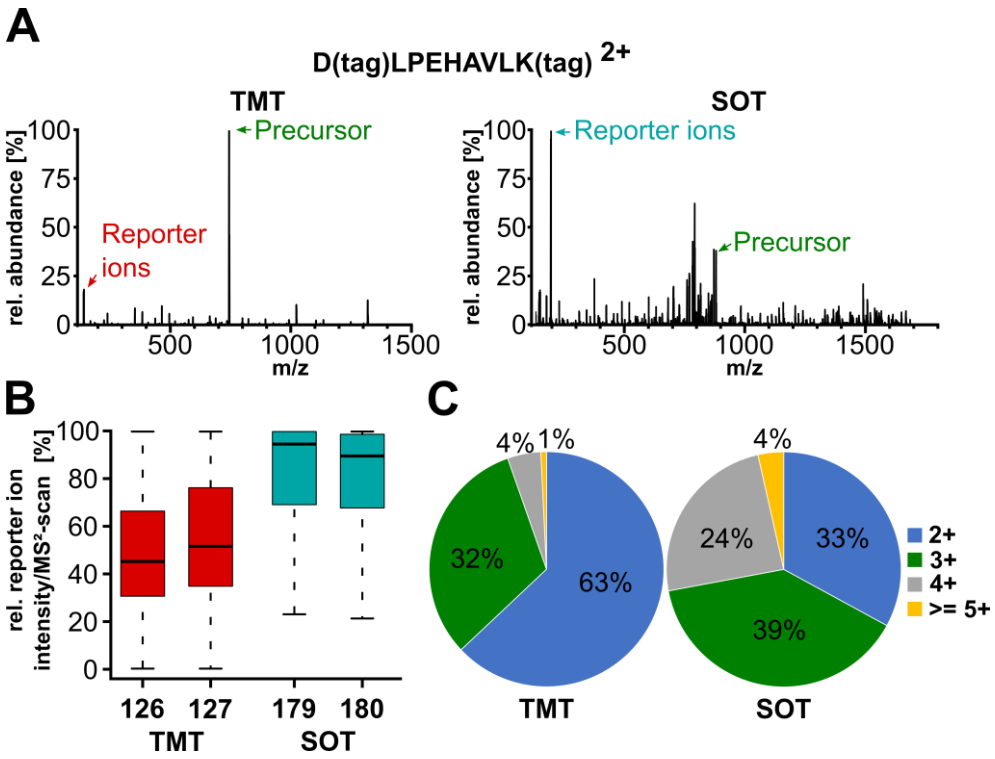

Figure 2. A) Comparison of fragmentation efficiency between TMT (**1**) and SOT (**2**) on a peptide. At a normalized collision energy of 28% HCD, the SOT-labelled peptide fragments more readily and yields high reporter ion signals. Tag = reacted reagent. B) Statistical analysis of the reporter ion relative intensities observed in the MS²-experiment. For SOT (**2**), the reporter ion exhibits an excellent visibility, facilitating reporter ion quantification. In comparison, TMT (**1**) produces reporter ions of lower intensity. C) Charge state distribution of precursor-peptides labelled with the TMT (**1**) or SOT (**2**) duplex. By using the SOT-reagent, higher charge states become more abundant, which should lead to more efficient fragmentation due to higher charge density.

While the reporter ion intensity allows measuring the relative ratios between peptides present in P-2^{180} versus P-2^{179}, it is desirable to quantify with the complementary ion clusters generated by the balancer-peptide conjugates.[16] Because these balancer-conjugates fragment further in the mass spectrometer, a large number of complementary ion clusters are formed, which can all be used for quantification. This provides higher data density and it reduces ratio distortion, because the complementary ions are sequence specific and are therefore distinguishable, unlike the reporter ions which are the same for all peptides. In our experiment, we observe that the SOT reagent **2** has ideal properties for such a complementary ion cluster analysis. When we studied the label-containing peptide fragment ions, we saw that 58% of these fragments still contained the intact reagent **2**, while 42% have lost the reporter group yielding complementary ion clusters (Fig. 3A).

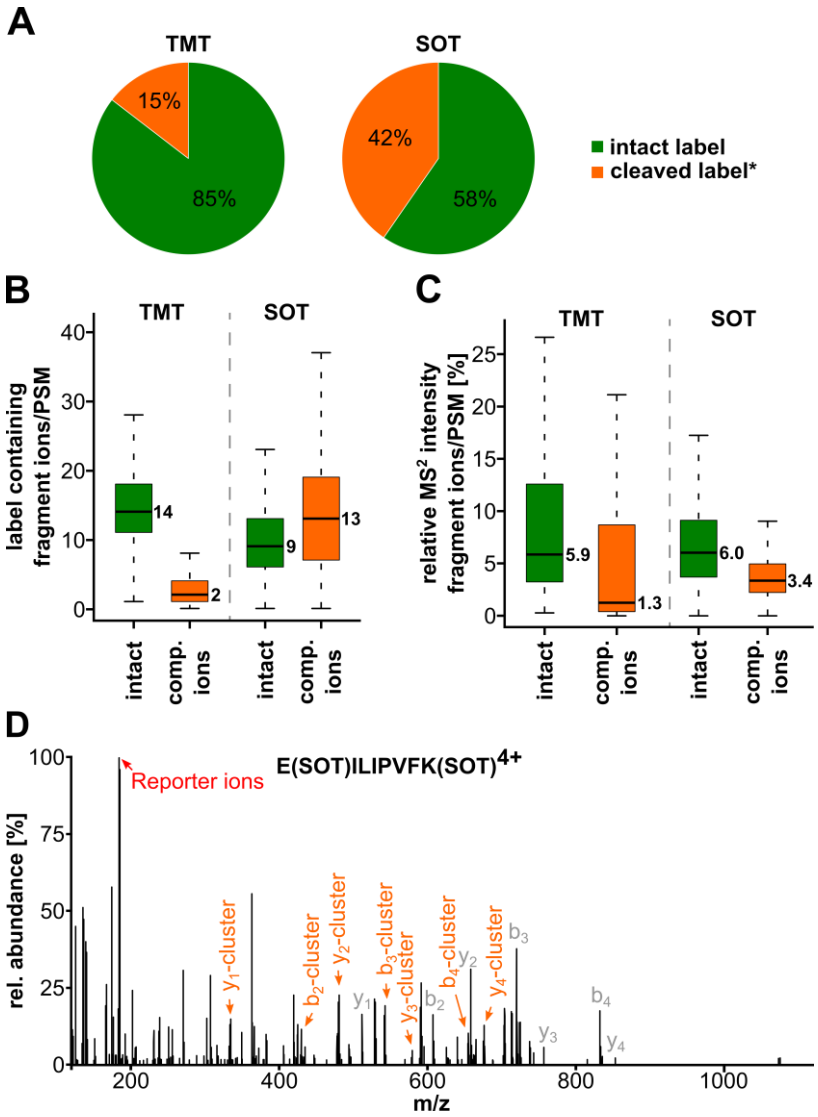

Figure 3. A) Ratio of all identified fragment ions containing either the intact label (reporter + balancer, green) or which show loss of the reporter ions, leading to the formation of complementary ion clusters (cleaved label, orange). *Because one intact label produces two cleaved labels in case of SOT (**2**) only, the amount of cleaved label containing fragments was divided by two to allow comparison with the TMT data. B) Statistical analysis of the quantity of labelled fragment ions per peptide spectral match (PSM). SOT-labelled peptides show a drastic increase in the number of complementary ions per spectrum compared to TMT-labelled peptides, resulting in 6–7 complementary ion clusters on average. C) Statistical analysis of the relative MS²-scan intensities of the labelled fragment ions per PSM. The median intensity of the complementary ions is elevated for SOT-labelled peptides when compared to the use of TMT. D) Example MS²-spectrum of the labelled peptide EILIPVFK^{4+}, depicting the reporter ions (red), seven complementary ion clusters (orange) and some fragment ions used for identification (grey).

This balanced ratio allows the parallel identification of the (intact) peptides with standard database search algorithms and quantification *via* the abundantly formed complementary ion clusters. In case of TMT, the amount of fragmentation is significantly lower and only 15% of all labelled fragment ions are cleaved. This holds true even when considering that the TMT-duplex complementary ions are indistinguishable, because they lose CO (containing the isotope marker) during fragmentation. Fig. 3B shows that the SOT reagent **2** creates on average 13 peptide-balancer fragments from every precursor for later quantification, which corresponds to 6–7 complementary ion clusters. For SOT-labelled peptides, there are not only more complementary ions compared to TMT-labelled peptides, but their median relative intensity in the respective MS²-spectra is also higher (Fig. 3C). An example spectrum is displayed in Fig. 3D. The signals for the reporter ions (red) and of seven complementary ion clusters (orange) are clearly visible with high relative intensities. For identification of the peptide, multiple high intensity ions are available (grey). Although the number of acquired MS²-scans was comparable for the SOT- and TMT-samples (42169 for SOT, 46062 for TMT), the peptide identification rate was lower for SOT-labelled peptides (20% for SOT, 35% for TMT).

To investigate whether our new reagent reduces the ratio distortion effect, we performed an experiment in which a 1:1 labelled mixture of HEK-lysate served as a background. Into this background, a labelled bovine serum albumin (BSA) digest was added in a 4:1 ratio in a low quantity (Fig. 4A). This ensures that only a small amount of BSA peptides gets selected for isolation and fragmentation in a large background of 1:1 labelled human peptides. This should give a large ratio distortion. As observed previously in similar datasets with strong distortion,[16] the normalized median reporter ion ratio for the BSA peptides is 1.15 in case of the SOT-sample and 1.11 in case of the TMT-sample, showing the massive distortion of the ratio towards 1:1 (Fig. 4B). We next studied the same SOT-dataset regarding the complementary ion clusters of the BSA peptides.

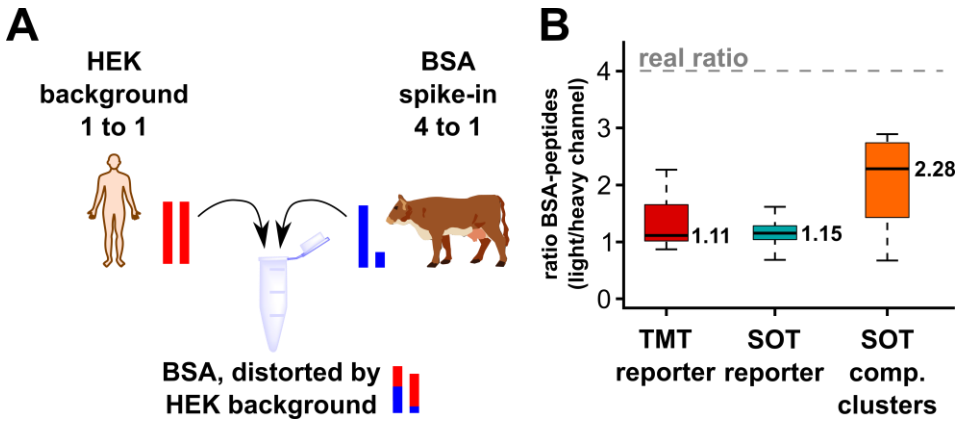

Figure 4. A) Experiment to show quantification of a protein with strong ratio distortion. HEK-lysate was labelled and mixed in a 1 to 1 ratio to serve as a background. Bovine serum albumin (BSA) was labelled and a 4 to 1 ratio was added into the background. Reporter ion intensities of BSA-peptides are highly distorted in the sample. B) Quantification results for measured BSA-peptides. Median reporter ion intensities of both TMT- and SOT-samples show a high distortion, leading to the impression of a nearly 1 to 1 ratio. Complementary ion cluster analysis results in a higher and therefore improved value of the BSA peptide ratio. Thus, SOT complementary ion cluster analysis reduces ratio distortion.

In 17 quantified peptides, 155 complementary ion clusters were detected and used for quantification. Analyzing their intensities provided a normalized median ratio of 2.3:1. The determined ratio is by a factor of 2 closer to the expected 4:1 ratio, showing the advantage of SOT complementary cluster analysis (SOT^{c}).

In summary, we report the design of a new isobaric labelling reagent that allows the efficient parallel formation of reporter ions and complementary ion clusters for peptide quantification. The reagent helps to reduce quantification errors caused by ratio distortion. Particularly attractive is the efficient formation of complementary ion clusters that results from fragmentations of the tag and the peptide backbone. These ion-clusters enable multiple quantification events per spectrum. Furthermore, due to the peptide-specific fragmentation, we expect the resulting quantifications to be even more robust against interference than when using the intact peptide complimentary ion cluster. This enables more accurate determination of relative peptide and hence protein abundances even in complex samples and might be particularly attractive for a targeted multiplexed approach.[20] The most important properties of the SOT reagent **2** are that reporter ions and complementary ion clusters are formed in parallel and that the introduction of multiple *tert*-amino groups generates the expected higher charge states which results in better peptide fragmentation. A current drawback is that the SOT reagent leads to identification of fewer peptides. The lower number is certainly caused by the currently available software, which is not yet optimized for the SOT reagent. In addition, the reagent increases the charge state, which could be another limiting factor. Software optimization and synthesis of a reagent that lacks the tertiary amine, can solve these problems. Research in this direction is ongoing.[21]

Acknowledgements

We thank the Deutsche Forschungsgemeinschaft for financial support *via* SPP1784, CA275 and GRK2062. We thank the Bundesministerium für Bildung und Forschung (BMBF) for additional support by the Excellence Cluster CiPS^{M}. Further support from the European Union through the Marie Curie International Training and Mobility Network “Clickgene” (grant No. 642023) is acknowledged M.S. thanks the Fonds der Chemischen Industrie for a predoctoral fellowship.

Keywords: Peptide derivatization reagent, sulfoxide pyrolysis, isobaric labelling, quantitative mass spectrometry, complementary ion clusters, proteomics

[1] S. Goodwin, J. D. McPherson, W. R. McCombie, *Nat. Rev. Genet.* **2016**, *17*, 333-351.
[2] M. Beck, A. Schmidt, J. Malmstroem, M. Claassen, A. Ori, A. Szymborska, F. Herzog, O. Rinner, J. Ellenberg, R. Aebersold, *Mol. Syst. Biol.* **2011**, *7*, 549.
[3] M.-S. Kim, S. M. Pinto, D. Getnet, R. S. Nirujogi, S. S. Manda, R. Chaerkady, A. K. Madugundu, D. S. Kelkar, R. Isserlin, S. Jain, J. K. Thomas, B. Muthusamy, P. Leal-Rojas, P. Kumar, N. A. Sahasrabuddhe, L. Balakrishnan, J. Advani, B. George, S. Renuse, L. D. N. Selvan, A. H. Patil, V. Nanjappa, A. Radhakrishnan, S. Prasad, T. Subbannayya, R. Raju, M. Kumar, S. K. Sreenivasamurthy, A. Marimuthu, G. J. Sathe, S. Chavan, K. K. Datta, Y. Subbannayya, A. Sahu, S. D. Yelamanchi, S. Jayaram, P. Rajagopalan, J. Sharma, K. R. Murthy, N. Syed, R. Goel, A. A. Khan, S. Ahmad, G. Dey, K. Mudgal, A. Chatterjee, T.-C. Huang, J. Zhong, X. Wu, P. G. Shaw, D. Freed, M. S. Zahari, K. K. Mukherjee, S. Shankar, A. Mahadevan, H. Lam, C. J. Mitchell, S. K. Shankar, P. Satishchandra, J. T. Schroeder, R. Sirdeshmukh, A. Maitra, S. D. Leach, C. G. Drake, M. K. Halushka, T. S. K. Prasad, R. H. Hruban, C. L. Kerr, G. D. Bader, C. A. Iacobuzio-Donahue, H. Gowda, A. Pandey, *Nature* **2014**, *509*, 575-581.
[4] N. Nagaraj, J. R. Wisniewski, T. Geiger, J. Cox, M. Kircher, J. Kelso, S. Pääbo, M. Mann, *Mol. Syst. Biol.* **2011**, *7*, 548.
[5] M. Uhlén, L. Fagerberg, B. M. Hallström, C. Lindskog, P. Oksvold, A. Mardinoglu, Å. Sivertsson, C. Kampf, E. Sjöstedt, A. Asplund, I. Olsson, K. Edlund, E. Lundberg, S. Navani, C. A.-K. Szigyarto, J. Odeberg, D. Djureinovic, J. O. Takanen, S. Hober, T. Alm, P.-H. Edqvist, H. Berling, H. Tegel, J. Mulder, J. Rockberg, P. Nilsson, J. M. Schwenk, M. Hamsten, K. von Feilitzen, M. Forsberg, L. Persson, F. Johansson, M. Zwahlen, G. von Heijne, J. Nielsen, F. Pontén, *Science* **2015**, *347*.
[6] E. F. Petricoin, K. C. Zoon, E. C. Kohn, J. C. Barrett, L. A. Liotta, *Nat. Rev. Drug Discovery* **2002**, *1*, 683-695.

[7] S.-E. Ong, B. Blagoev, I. Kratchmarova, D. B. Kristensen, H. Steen, A. Pandey, M. Mann, *Mol. Cell. Proteomics* **2002**, *1*, 376-386.
[8] S.-E. Ong, M. Mann, *Nat. Protoc.* **2007**, *1*, 2650-2660.
[9] J. Cox, M. Y. Hein, C. A. Luber, I. Paron, N. Nagaraj, M. Mann, *Mol. Cell. Proteomics* **2014**, *13*, 2513-2526.
[10] A. Thompson, J. Schäfer, K. Kuhn, S. Kienle, J. Schwarz, G. Schmidt, T. Neumann, C. Hamon, *Anal. Chem.* **2003**, *75*, 1895-1904.
[11] T. Werner, I. Becher, G. Sweetman, C. Doce, M. M. Savitski, M. Bantscheff, *Anal. Chem.* **2012**, *84*, 7188-7194.
[12] T. Köcher, P. Pichler, M. Schutzbier, C. Stingl, A. Kaul, N. Teucher, G. Hasenfuss, J. M. Penninger, K. Mechtler, *J. Proteome Res.* **2009**, *8*, 4743-4752.
[13] C. T. Mant, R. S. Hodges, *Methods Enzymol.* **1996**, *271*, 3-50.
[14] Y. Dunayevskiy, P. Vouros, T. Carell, E. A. Wintner, J. Rebek, *Anal. Chem.* **1995**, *67*, 2906-2915.
[15] Y. M. Dunayevskiy, P. Vouros, E. A. Wintner, G. W. Shipps, T. Carell, J. Rebek, *Proc. Natl. Acad. Sci. U. S. A.* **1996**, *93*, 6152-6157.
[16] M. Wühr, W. Haas, G. C. McAlister, L. Peshkin, R. Rad, M. W. Kirschner, S. P. Gygi, *Anal. Chem.* **2012**, *84*, 9214-9221.
[17] S. Y. Ow, M. Salim, J. Noirel, C. Evans, I. Rehman, P. C. Wright, *J. Proteome Res.* **2009**, *8*, 5347-5355.
[18] N. A. Kulak, G. Pichler, I. Paron, N. Nagaraj, M. Mann, *Nat. Methods* **2014**, *11*, 319-324.
[19] J. Cox, M. Mann, *Nat. Biotechnol.* **2008**, *26*, 1367-1372.
[20] B. K. Erickson, C. M. Rose, C. R. Braun, A. R. Erickson, J. Knott, G. C. McAlister, M. Wühr, J. A. Paulo, R. A. Everley, S. P. Gygi, *Mol. Cell* **2017**, *65*, 361-370.
[21] For a sample of the new reagent **2** and the in house software package used to analyze the data please visit our homepage at www.carellgroup.de and contact us.

Supporting Information

I. General information

Unless noted otherwise, all reactions were performed using oven-dried glassware under an atmosphere of argon. Molsieve-dried solvents were used from *Sigma Aldrich* and chemicals were bought from *Sigma Aldrich*, *TCI*, *Carbolution, Roth* and *Carbosynth*. Formaldehyde-^{13}C solution (20wt% in water, 99 atom% ^{13}C) and bromoacetic acid-2-^{13}C (99 atom% ^{13}C) were purchased from *Sigma Aldrich*. HyperSep™ C18 cartridges for desalting were purchased from *ThermoFisher Scientific.* For extraction and chromatography purposes, technical grade solvents were distilled prior to their usage. Reaction controls were performed using TLC-Plates from *Merck* (Merck 60 F^{254}), flash column chromatography purifications were performed on *Merck* Geduran Si 60 (40–63 μM). Visualization of the TLC plates was achieved through UV-absorption or through staining with *CAM stain* (Cerium ammonium molybdate stain). NMR spectra were recorded in deuterated solvents on *Varian VXR400S*, *Varian Inova 400*, *Bruker AMX 600*, *Bruker Ascend 400* and *Bruker Avance III HD*. HR-ESI-MS spectra were obtained from a *Thermo Finnigan* LTQ FT-ICR. IR-measurements were performed on a *Perkin Elmer Spectrum BX FT-IR* spectrometer with a diamond-ATR *(Attenuated Total Reflection)* unit.

II. Synthesis of starting materials

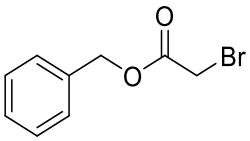

Benzyl bromoacetate (12)

General procedure 1 (GP1): In a dry and Ar-flushed Schlenk-flask, bromoacetic acid (1.00 g, 7.19 mmol, 1.2 equiv), phenylmethanol (640 µL, 6.20 mmol, 1.0 equiv) and 4-methylbenzene-1-sulfonic acid (21 mg, 0.12 mmol, 0.02 equiv) were dissolved in 10 mL toluene and refluxed for 2 h. After completion, the reaction mixture was cooled to rt and washed with 20% sodium bicarbonate solution in water (2 x 20 mL) followed by brine (2 x 20 mL) and water (2 x 20 mL). The combined organic layers were dried over magnesium sulfate and concentrated *in vacuo.* Purification by flash column chromatography (silica gel, EtOAc/DCM 1:4) yielded **12** as a colourless oil (1.38 g, 6.02 mmol, 84%).

^{1}H-NMR (400 MHz, methanol-d_4) δ = 7.46 – 7.13 (m, 5H), 5.16 (s, 2H), 3.95 (s, 2H) *ppm*.

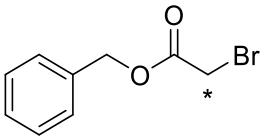

Benzyl bromo(2-^{13}C)acetate (11)

Following **GP1**, bromoacetic acid-2-^{13}C (500 mg, 3.60 mmol, 1.2 equiv) and phenylmethanol (320 µL, 3.10 mmol, 1.0 equiv) were dissolved in toluene (5 mL). 4-Methylbenzene-1-sulfonic acid (11 mg, 60 µmol, 0.02 equiv) was added and the reaction mixture was stirred under reflux for 2 h. Work-up was performed as described under **GP1**. Purification by flash column chromatography (silica gel, EtOAc/DCM 1:4) yielded **11** as a colourless oil (427 mg, 1.86 mmol, 52%).

^{1}H-NMR (400 MHz, methanol-d_4) δ = 7.41 – 7.33 (m, 5H), 5.20 (s, 2H), 4.18 (s, 1H), 3.80 (s, 1H) *ppm*. **HRMS** (EI): calc. for $C_8{}^{13}CH_{10}BrO_2^{\cdot+}$ $[M]^{\cdot+}$: 229.9820; found: 229.9718 *m/z*. **IR** (cm^{-1}): $\tilde{\nu}$ = 3065, 1733, 1587, 1497, 1455, 1376, 1278, 1213, 1147, 1106, 967, 736.

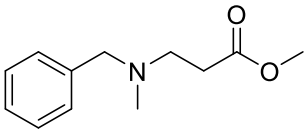

Methyl 3-[benzyl(methyl)amino]propanoate (13)

Methyl-3-bromopropanoate (3.00 g, 18.0 mmol, 1.0 equiv) and N-methyl-1-phenylmethanamine (2.18 g, 18.0 mmol, 1.0 equiv) were dissolved in acetonitrile (120 mL). After 2 min stirring at rt, Na_2CO_3 (19.0 g, 180 mmol, 10.0 equiv) was added and the temperature was increased to 70 °C for 24 h. After cooling, the reaction solution was filtered, and DCM (120 mL) was added to the filtrate. The organic phase was washed with 0.5 M NaOH (3 × 50 mL) and dried over Na_2SO_4. After filtration, the product was concentrated under reduced pressure to yield **13** as colourless oil (3.44 g, 16.5 mmol, 92%).[1]

^{1}H-NMR (400 MHz, $CDCl_3$): δ = 7.30 − 7.18 (m, 5H), 3.63 (s, 3H), 3.48 (s, 2H), 2.71 (t, *J* = 7.2 Hz, 2H) 2.49 (t, *J* = 7.2 Hz, 2H), 2.17 (s, 3H) *ppm*. **^{13}C-NMR** (101 MHz, $CDCl_3$): δ = 173.0, 138.9, 128.9, 128.2, 127.0, 62.1, 52.6, 51.6, 41.9, 32.8 *ppm*. **HRMS** (ESI): calc. for $C_{12}H_{18}NO_2^+$ $[M+H]^+$: 208.1332; found: 208.1331 *m/z*. **IR** (cm^{-1}): $\tilde{\nu}$ = 2950 (w), 2841 (w), 2790 (w), 1737 (s), 1495 (w), 1452 (m), 1236 (m), 1357 (w), 1325 (w), 1202 (m), 1168 (s), 1125 (m), 1975 (w), 1038 (m), 1025 (m).

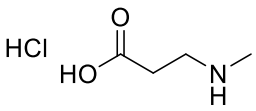

3-(Methylamino)propanoic acid hydrochloride (14)

In a flame-dried Schlenk tube methyl 3-[benzyl(methyl)amino]propanoate **13** (1.00 g, 4.82 mmol, 1.0 equiv) was dissolved in MeOH (60 mL). Then the atmosphere of the tube was purged with N_2 and Pd/C (100 mg, 10wt%) was added in small portions to the solution. The reaction was stirred for 16 h at room temperature in an H_2 atmosphere. Pd/C was filtered off through celite. Evaporation resulted in a yellowish oil. The crude volatile product was used without further purification for the next step. The resulting methyl ester was dissolved in 5 M HCl and refluxed for 8 h. The solution was evaporated to dryness. Recrystallization from MeOH/Et_2O yielded the desired product **14** as colourless hygroscopic crystals (478 mg, 3.42 mmol, 71%).[1]

Mp.: 89 − 92 °C. **^{1}H-NMR** (400 MHz, D_2O) δ = 3.28 (t, J = 6.4 Hz, 2H), 2.81 (t, J = 6.5 Hz, 2H), 2.72 (s, 3H) *ppm*. **^{13}C-NMR** (101 MHz, $CDCl_3$): δ = 174.1, 44.4, 33.0, 29.9 *ppm*. **HRMS** (ESI): calc. for $C_4H_{10}NO_2^+$ $[M+H]^+$: 104.0706; found: 104.0706 *m/z*. **IR** (cm^{-1}): $\tilde{\nu}$ = 3376 (w), 2968 (s), 2819 (s), 1729 (s), 1557 (w) 1465 (m), 1402 (s) 1351 (w), 1289 (w), 1189 (s), 1156 (s), 1024 (s).

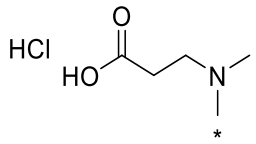

3-{Methyl[(^{13}C)methyl]amino}propanoic acid hydrochloride (10)

3-(Methylamino)propanoic acid hydrochloride **14** (401 mg, 2.87 mmol, 1.0 equiv) was dissolved in 88% formic acid (1.79 mL, 44.8 mmol, 15.6 equiv). Then (^{13}C)formaldehyde (20% in water; 1.00 g, 6.45 mmol, 2.3 equiv) was added and the solution was heated *via* microwave irridation (110 °C, 100 W, 1 h). Conc. HCl (200 µL) was added and the solvent was removed *in vacuo*. Traces of formic acid were removed azeotropically with toluene *in vacuo*. The slightly yellowish solid was recrystallized from MeOH/Et_2O to obtain a colourless solid (383 mg, 2.48 mmol, 86%).[2-4]

Mp.: 183 °C. **^{1}H-NMR** (400 MHz, D_2O): δ = 3.30 (td, J = 6.7, 3.0 Hz, 2H), 2.97 – 2.60 (m, 8H) *ppm*. **^{13}C-NMR** (101 MHz, D_2O): δ = 174.1, 53.1, 43.3, 42.8, 28.8 *ppm*. **HRMS** (ESI): calc. for $C_4{}^{13}CH_{12}NO_2^+$ $[M+H]^+$ 119.0896, found 119.0896 *m/z*. **IR** (cm^{-1}): $\tilde{\nu}$ = 2957(m), 2692 (m), 2592 (w), 2481 (w), 1717 (s), 1468 (w), 1420 (m), 1370 (w), 1300 (w), 1201 (s) 1161 (m), 1006 (w), 966 (m), 854 (s), 798 (m).

III. General experimental procedures

In the following section, molecules towards compound 2[179] will be assigned with ** and molecules towards compound 2[180] will be assigned with *.

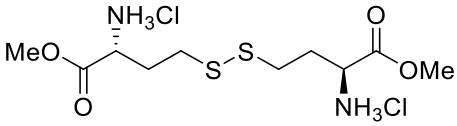

Methyl (2*R*)-2-amino-4-{[(3*S*)-3-amino-4-methoxy-4-oxobutyl]disulfanyl} butanoate hydrochloride (3)

In a dry and Ar-flushed 250 mL Schlenk-flask, DL-homocystine (4,4'-disulfanediylbis(2-aminobutanoic acid) (6.00 g, 22.3 mmol, 1.0 equiv) was dissolved in anhydrous MeOH (80 mL). The colourless suspension was cooled to 0 °C and thionyl chlorid (6.48 mL, 89.4 mmol, 4.0 equiv) was added dropwise *via* syringe. The resulting colourless reaction mixture was allowed to warm to rt over 3 h. Then, the reaction mixture was concentrated *in vacuo* yielding **3** as a colourless solid (8.24 g, 22.3 mmol, quant).

^{1}H-NMR (400 MHz, methanol-d_4) δ = 4.21 (t, J = 6.5 Hz, 2H), 3.86 (s, 6H), 2.84 (m, 4H), 2.47 – 2.22 (m, 4H) *ppm*. **^{13}C-NMR** (400 MHz, methanol-d_4) δ = 170.5, 53.9, 52.6, 33.6, 30.9 *ppm*. **HRMS** (ESI): calc. for $C_{10}H_{21}N_2O_4S_2^+$ $[M+H]^+$: 297.0937; found: 297.0938 *m/z*. **IR** (cm^{-1}): $\tilde{\nu}$ = 3373, 2854, 2611, 2003, 1738, 1591, 1503, 1439, 1224, 1139, 860.

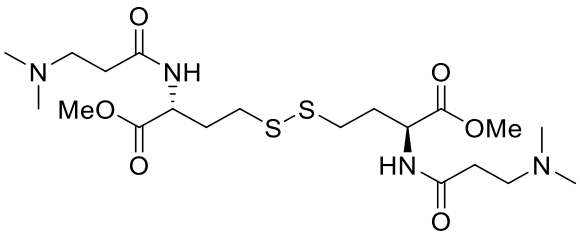

Methyl (2*R*)-2-[3-(dimethylamino)propanamido]-4-({(3*S*)-3-[3-(dimethylamino)propanamido]-4-methoxy-4-oxobutyl}disulfanyl)butanoate (4)

General procedure 2 (GP2): In a dry and Ar-flushed Schlenk-flask, 3-(dimethylamino)propanoic acid dihydrochloride (372 mg, 2.42 mmol, 2.4 equiv) and the methyl ester **3** (300 mg, 1.01 mmol, 1.0 equiv) were dissolved in 5 mL anhydrous DMF. Then, triethylamine (491 µL, 2.12 mmol, 3.5 equiv), HOBt (340 mg, 2.50 mmol, 2.5 equiv) and EDC*HCl (405 mg, 2.61 mmol, 2.6 equiv) were added and stirred for

2 h at 60 °C. The resulting orange suspension was concentrated *in vacuo.* Purification by flash column chromatography (silica gel, DCM/MeOH 16:1) furnished **4** as a colourless solid (426 mg, 861 µmol, 86%).

^{1}H-NMR (800 MHz, methanol-d_4) δ = 4.62 – 4.55 (m, 2H), 3.75 (d, J = 1.5 Hz, 3H), 3.37 (s, 3H), 2.84 – 2.79 (m, 2H), 2.78 – 2.72 (m, 2H), 2.71 – 2.63 (m, 4H), 2.46 (td, J = 7.3, 2.8 Hz, 4H), 2.30 – 2.04 (m, 16H) *ppm*. **^{13}C-NMR** (201 MHz, methanol-d_4) δ = 174.4, 173.5, 52.9, 52.4, 49.9, 35.6, 35.5, 34.1, 32.1 *ppm*. **HRMS** (ESI): calc. for $C_{20}H_{39}N_4O_6S_2^+$ $[M+H]^+$: 495.2305; found: 495.2303 *m/z*. **IR** (cm^{-1}): $\tilde{\nu}$ = 3382, 2953, 2833, 2498, 2069, 1733, 1643, 1548, 1439, 1222, 1173, 1119, 977, 856.

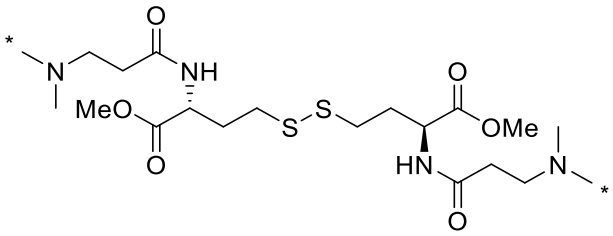

Dimethyl-4,4'-disulfanediyl(2*R*,2'*S*)-bis(2-(3-(methyl(methyl-^{13}C)amino)-propanamido)-butanoate) (4)**

Following **GP2** 3-{methyl[(^{13}C)methyl]amino}propanoic acid hydrochloride **10** (220 mg, 1.42 mmol, 2.2 equiv) and methyl ester **3** (238 mg, 645 µmol, 1.0 equiv) yielded **4**** as a colourless solid (200 mg, 403 µmol, 62%).

^{1}H-NMR ($CDCl_3$, 400 MHz): δ = 4.57 (ddd, J = 8.5, 4.8, 3.1 Hz, 2H), 3.73 (s, 6H), 2.83 − 2.59 (m, 8H), 2.46 − 1.99 (m, 20H). **HRMS** (ESI): calc. for $C_{18}{}^{13}C_2H_{39}N_4O_6S_2^+$ $[M+H]^+$: 497.2373; found: 497.2379 *m/z*.

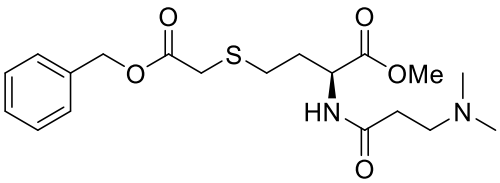

Methyl (2*S*)-4-{[2-(benzyloxy)-2-oxoethyl]sulfanyl}-2-[3-(dimethylamino)propanamido]butanoate (5)

General procedure 3 (GP3): Disulfide **4** (750 mg, 1.51 mmol, 1.0 equiv) was dissolved in a mixture of 5 mL H_2O and 15 mL DMF. Then, $NaHCO_3$ (535 mg, 6.37 mmol, 4.2 equiv) and TCEP*HCl (435 mg, 1.51 mmol, 1.0 equiv) were added to

the reaction mixture under argon. The reduction was monitored by LC-MS and TLC. After completion of the reduction, benzyl bromoacetate (600 µL, 3.79 mmol, 2.5 equiv) was added and the reaction mixture was stirred for 2 h at rt. The reaction mixture was then concentrated *in vacuo* and purified by flash column chromatography (silica gel, 5% MeOH in DCM) furnishing **5** as a colourless oil (510 mg, 1.29 mmol, 42%).

^{1}H-NMR (400 MHz, methanol-d_4) δ = 7.53 – 7.15 (m, 5H), 5.18 (s, 2H), 4.56 (dd, *J* = 8.9, 4.8 Hz, 1H), 3.71 (s, 3H), 3.33 (s, 2H), 2.75 – 2.58 (m, 4H), 2.45 (t, *J* = 7.2 Hz, 2H), 2.29 (s, 6H), 2.17 – 2.05 (m, 1H), 2.02 – 1.90 (m, 1H) *ppm*.

^{13}C-NMR (151 MHz, $CDCl_3$) δ = 172.6, 172.5, 170.2, 135.6, 128.7, 128.5, 128.4, 67.2, 55.1, 52.5, 51.1, 44.6, 33.5, 32.8, 31.8, 28.5 *ppm*. **HRMS** (ESI): calc. for $C_{19}H_{29}N_2O_5S^+$ $[M+H]^+$: 397.1791; found: 397.1791 *m/z*. **IR** (cm^{-1}): ṽ = 3285, 2950, 2864, 1736, 1655, 1539, 1455, 1440, 1374, 1271, 1213, 1170, 1146, 1025, 748, 698.

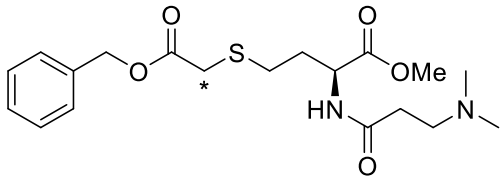

Methyl (2*S*)-4-{[2-(benzyloxy)-2-oxo(1-^{13}C)ethyl]sulfanyl}-2-[3-(dimethylamino)propanamido]butanoate (5*)

Following **GP3**, the disulfide **4** (370 mg, 750 µmol, 1.0 equiv) and benzyl bromo(2-^{13}C)acetate **11** (294 µL, 1.86 mmol, 2.3 equiv) gave **5*** as a colourless oil (550 mg, 1.38 mmol, 92%).

^{1}H-NMR (400 MHz, methanol-d_4) δ = 7.42 – 7.28 (m, 5H), 5.16 (s, 2H), 4.59 – 4.52 (m, 1H), 3.70 (s, 3H), 3.50 (s, 1H), 3.15 (s, 1H), 2.93 (t, *J* = 7.0 Hz, 2H), 2.75 – 2.60 (m, 2H), 2.56 (t, *J* = 7.0 Hz, 2H), 2.50 (s, 6H), 2.19 – 2.05 (m, 1H), 2.04 – 1.86 (m, 1H) *ppm*. **HRMS** (ESI): calc. for $C_{18}{}^{13}CH_{29}N_2O_5S^+$ $[M+H]^+$: 398.1825; found: 398.1824 *m/z*.

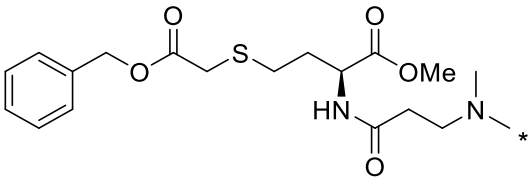

Methyl (2*S*)-4-{[2-(benzyloxy)-2-oxoethyl]sulfanyl}-2-(3-{methyl[(^{13}C)methyl]amino}propanamido)butanoate (5)**

Following **GP3**, the disulfide **4**** (200 mg, 400 µmol, 1.0 equiv) furnished **5**** as a colourless oil (252 mg, 634 µmol, 79%).

^{1}H-NMR (400 MHz, methanol-d_4): δ = 7.40 − 7.28 (m, 5H), 5.15 (s, 2H), 4.53 (dd, *J* = 8.93, 4.90 Hz, 1H), 3.69 (s, 3H), 3.32 (s, 2H), 2.73 – 2.56 (m, 4H), 2.44 – 1.87 (m, 10H) *ppm*. **^{13}C-NMR** (101 MHz, methanol-d_4) δ = 174.5, 173.6, 172.0, 137.3, 129.6, 129.3, 129.3, 67.9, 56.0, 52.8, 52.6, 45.1, 34.2, 34.0, 32.0, 29.5 *ppm*. **HRMS** (ESI): calc. for $C_{18}{}^{13}CH_{29}N_2O_5S^+$ $[M+H]^+$: 398.1825; found: 398.1826 *m/z*.

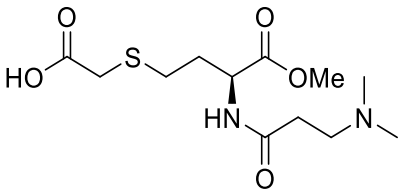

({(3*S*)-3-[3-(Dimethylamino)propanamido]-4-methoxy-4-oxobutyl}sulfanyl)acetic acid (6)

General procedure 4 (GP4): In a dry and Ar-flushed Schlenk-flask, the benzyl-protected sulfide **5** (160 mg, 400 µmol, 1.0 equiv) was dissolved in 3 – 4 mL of 10 % formic acid in methanol. Then, palladium black (160 mg, 100wt%) was added to the reaction mixture and stirred for 2 h at 40 °C. The deprotection was monitored by LC-MS and TLCs. After completion, the reaction mixture was filtered, concentrated *in vacuo* and purified by flash column chromatography (silica gel, 25 % MeOH in DCM) furnishing **6** as a colourless oil (100 mg, 326 µmol, 81%).

^{1}H-NMR (400 MHz, methanol-d_4) δ = 4.61 (dd, *J* = 9.4, 4.2 Hz, 1H), 3.27 (t, *J* = 6.8 Hz, 3H), 3.21 (t, *J* = 6.5 Hz, 1H), 3.12 (s, 2H), 2.75 (s, 6H), 2.73 – 2.55 (m, 4H), 2.18 – 2.07 (m, 1H), 2.05 – 1.93 (m, 1H) *ppm*. **LRMS (ESI$^+$)**: calc. for $C_{12}H_{23}N_2O_5S^+$ $[M+H]^+$: 307.1322; found: 307.10 *m/z*. **IR** (cm^{-1}): $\tilde{\nu}$ = 3253, 1734, 1652, 1574, 1468, 1372, 1217, 1147, 1084, 977, 761.

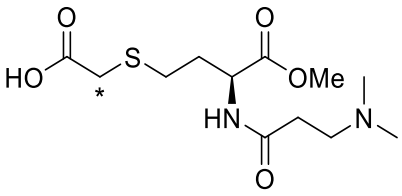

({(3*S*)-3-[3-(Dimethylamino)propanamido]-4-methoxy-4-oxobutyl}sulfanyl)(2-^{13}C)acetic acid (6*)

Following **GP4**: **5*** (580 mg, 1.46 mmol, 1.0 equiv) gave **6*** as a colourless oil (280 mg, 911 µmol, 62%).

^{1}H-NMR (400 MHz, methanol-d_4) δ = 4.62 (dd, J = 9.4, 4.2 Hz, 1H), 3.72 (s, 3H), 3.35 (s, 2H), 3.30 – 3.24 (m, 2H), 3.17 (dq, J = 13.0, 6.4 Hz, 1H), 2.74 (s, 6H), 2.72 – 2.60 (m, 4H), 2.18 – 1.94 (m, 2H) *ppm*. **^{13}C-NMR** (101 MHz, methanol-d_4) δ = 173.9, 172.4, 170.2, 55.2, 52.8, 49.8, 44.0, 37.3, 31.8, 31.6, 29.2 *ppm*. **HRMS** (ESI): calc. for $C_{11}{}^{13}CH_{23}N_2O_5S^+$ $[M+H]^+$: 308.1356; found: 308.1356 *m/z*.

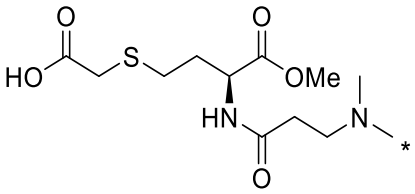

{[(3*S*)-4-Methoxy-3-(3-{methyl[(^{13}C)methyl]amino}propanamido)-4-oxobutyl]sulfanyl}acetic acid (6)**

Following **GP4**: **5**** (252 mg, 630 µmol, 1.0 equiv) furnished **6**** as a colourless oil (181 mg, 589 µmol, 93%).

^{1}H-NMR (400 MHz, methanol-d_4): δ = 4.61 (dd, J = 9.5, 4.2 Hz, 1H), 3.70 (s, 3H), 3.38 – 3.16 (m, 4H), 3.08 (d, J = 3.26 Hz, 2H), 2.94 – 2.59 (s, 10H) *ppm*. **HRMS** (ESI): calc. for $C_{11}{}^{13}CH_{23}N_2O_5S^+$ $[M+H]^+$: 308.1356; found 308.1357 *m/z*.

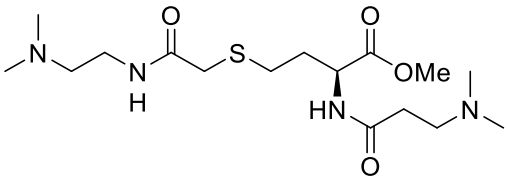

Methyl (2*S*)-4-[(2-{[2-(dimethylamino)ethyl]amino}-2-oxoethyl)sulfanyl]-2-[3-(dimethylamino)propanamido]butanoate (7)

Genral procedure 5 (GP5): The acid **6** (100 mg, 330 µmol, 1.0 equiv) was placed in a dry and Ar-flushed 50 mL Schlenk-flask and dissolved in 10 mL of dry DMF. Then N^1,N^2-dimethylethane-1,2-diamine (42.0 µL, 390 µmol, 1.2 equiv), diisopropylethylamine (83.0 µL, 490 µmol, 1.5 equiv) and PyBOP (203 mg, 39.0 µmol, 1.2 equiv) were added and the reaction mixture was stirred at rt for 1 h. The reaction mixture was concentrated *in vacuo* and purified by flash column chromatography (silica gel, 1:12 MeOH/DCM) furnishing **7** as a colourless oil (90.0 mg, 239 µmol, 73%).

^{1}H-NMR (400 MHz, methanol-d_4) δ = 4.56 (dd, *J* = 9.0, 4.8 Hz, 1H), 3.72 (s, 3H), 3.38 – 3.32 (m, 2H), 3.19 (d, *J* = 1.3 Hz, 2H), 2.74 – 2.57 (m, 4H), 2.47 (dt, *J* = 11.6, 6.8, 4H), 2.30 (d, *J* = 4.3 Hz, 12H), 2.12 (dddd, *J* = 13.2, 8.3, 7.2, 4.9 Hz, 1H), 2.03 – 1.92 (m, 1H) *ppm*. **^{13}C-NMR** (101 MHz, methanol-d_4) δ = 174.4, 173.6, 172.5, 59.0, 56.0, 52.8, 52.6, 45.4, 45.0, 38.2, 36.0, 34.0, 32.1, 29.7 *ppm*. **LRMS (ESI$^+$)**: calc. for $C_{16}H_{33}N_4O_4S^+$ $[M+H]^+$: 377.2217; found: 377.19 *m/z*. **IR** (cm^{-1}): $\tilde{\nu}$ = 3375, 2878, 17740, 1597, 1509, 1439, 1226, 1144, 1066, 1022, 903, 843, 744.

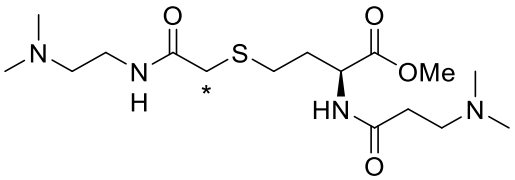

Methyl (2*S*)-4-{[2-{[2-(dimethylamino)ethyl]amino}-2-oxo(1-^{13}C)ethyl]sulfanyl}-2-[3-(dimethylamino)propanamido]butanoate (7*)

Following **GP5**, **6*** (270 mg, 870 µmol, 1.0 equiv) furnished **7*** as a colourless oil (246 mg, 652 µmol, 74%).

^{1}H-NMR (400 MHz, methanol-d_4) δ = 4.56 (dd, *J* = 9.0, 4.8 Hz, 1H), 3.72 (s, 3H), 3.36 – 3.33 (m, 4H), 2.74 – 2.58 (m, 4H), 2.47 (dt, *J* = 11.4, 7.0 Hz, 4H), 2.30 (d, *J* = 4.1 Hz,

12H), 2.18 – 1.92 (m, 1H), 1.29 – 1.15 (m, 1H) *ppm*. **LRMS (ESI$^+$)**: calc. for $C_{15}{}^{13}CH_{33}N_4O_4S^+$ $[M+H]^+$: 378.2251; found: 378.24 *m/z*.

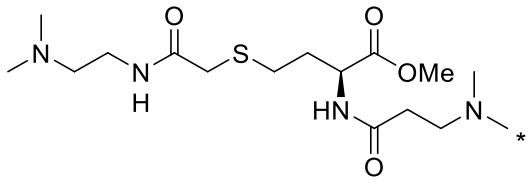

Methyl (2*S*)-4-[(2-{[2-(dimethylamino)ethyl]amino}-2-oxoethyl)sulfanyl]-2-(3-{methyl[(^{13}C)methyl]amino}propanamido)butanoate (7)**

Following **GP5, 6**** (181 mg, 590 µmol, 1.0 equiv) furnished **7**** as a colourless oil (173 mg, 458 µmol, 78%).

^{1}H-NMR (400 MHz, methanol-d_4): δ = 4.46 (dd, *J* = 9.0, 4.8 Hz, 1H), 3.62 (s, 3H), 3.25 (t, *J* = 6.95 Hz, 2H), 3.09 (s, 2H), 2.66 – 2.48 (m, 4H), 2.44 – 1.80 (m, 18H) *ppm*. **^{13}C-NMR** (101 MHz, methanol-d_4): δ = 172.9, 172.3, 171.1, 57.6, 54.6, 51.5, 51.3, 44.0, 43.6, 36.8, 34.6, 34.2, 32.5, 30.7, 28.3 *ppm*. **HRMS** (ESI): calc. for $C_{15}{}^{13}CH_{33}N_4O_4S^+$ $[M+H]^+$: 378.2251; found 378.2252 *m/z*.

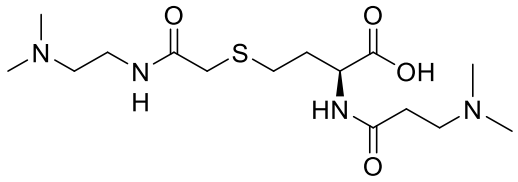

(2*S*)-4-[(2-{[2-(Dimethylamino)ethyl]amino}-2-oxoethyl)sulfanyl]-2-[3-(dimethylamino)propanamido]butanoic acid (8)

General procedure 6 (GP6): The methylester **7** (90.0 mg, 240 µmol, 1.0 equiv) was dissolved in a mixture of 2 mL H_2O and 5 mL MeOH. Then LiOH (17.0 mg, 710 µmol, 3.0 equiv) was added and the reaction mixture was stirred at rt for 1 h. The product was concentrated under reduced pressure and then desalted with HyperSep™ C18 cartridges (equilibrate: 15 mL acetonitrile and 10 mL H_2O; load: 25 mg in 0.3 mL water; wash: 0.5 mL water; elute: 6 mL 4:1 acetonitrile/water). Lyophilization furnished **8** as a colourless solid (87 mg, 240 µmol, quant.).

^{1}H-NMR (400 MHz, methanol-d_4) δ = 4.55 (dd, *J* = 9.3, 4.5 Hz, 1H), 3.64 (t, *J* = 5.9 Hz, 2H), 3.46 (t, *J* = 6.7 Hz, 2H), 3.35 (t, *J* = 6.0 Hz, 2H), 2.95 (d, *J* = 13.2 Hz, 12H), 2.90 – 2.83 (m, 2H), 2.81 – 2.64 (m, 2H), 2.22 – 2.11 (m, 1H), 2.09 – 1.97 (m,

1H) *ppm*. **^{13}C-NMR** (101 MHz, methanol-d_4) δ = 174.8, 173.7, 171.9, 58.0, 54.9, 52.7, 43.9, 43.7, 36.2, 36.0, 32.1, 30.8, 30.1 *ppm*. **HRMS** (ESI): calc. for $C_{15}H_{29}N_4O_4S^-$ [M-H]$^-$: 361.1915; found: 361.1919 *m/z*. **IR** (cm^{-1}): $\tilde{\nu}$ = 3368, 2916, 1743, 1632, 1524, 1439, 1311, 1227, 1160, 1059, 984, 845.

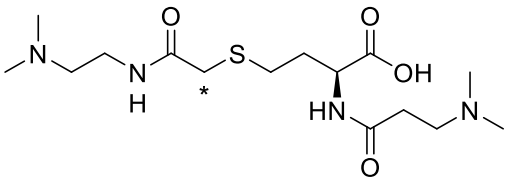

(2*S*)-4-{[2-{[2-(Dimethylamino)ethyl]amino}-2-oxo(1-^{13}C)ethyl]sulfanyl}-2-[3-(dimethylamino)propanamido]butanoic acid (8*)

Following **GP6**: **7*** (220 mg, 580 µmol, 1.0 equiv) furnished **8*** as a colourless solid (110 mg, 289 µmol, 74%).

^{1}H-NMR (400 MHz, methanol-d_4) δ = 4.33 (dd, *J* = 7.8, 4.6 Hz, 1H), 3.39 – 3.02 (m, 4H), 2.67 – 2.56 (m, 4H), 2.45 (dt, *J* = 14.7, 7.1 Hz, 4H), 2.27 (d, *J* = 3.2, 12H), 2.18 – 1.87 (m, 2H) *ppm*. **^{13}C-NMR** (101 MHz, methanol-d_4) δ = 176.8, 172.3, 172.3, 57.6, 54.8, 54.2, 44.1, 43.7, 37.0, 36.9, 33.2, 32.7, 28.6 *ppm*. **HRMS** (ESI): calc. for $C_{14}{}^{13}CH_{29}N_4O_4S^-$ [M-H]$^-$: 362.1949; found: 362.1952 *m/z*.

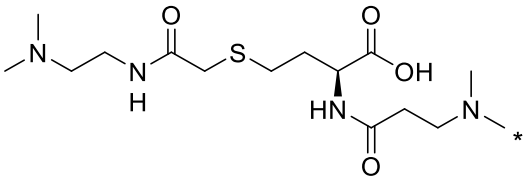

(2*S*)-4-[(2-{[2-(Dimethylamino)ethyl]amino}-2-oxoethyl)sulfanyl]-2-(3-{methyl[(^{13}C)methyl]amino}propanamido)butanoic acid (8)**

Following **GP6**: **7**** (173 mg, 0.460 mmol, 1.0 equiv) furnished **8**** as a colourless solid (105 mg, 289 µmol, 62%).

^{1}H NMR (400 MHz, methanol-d_4): δ = 4.33 (dd, *J* = 7.8, 4.6 Hz, 1H), 3.35 (t, *J* = 6.41 Hz, 2H), 3.19 (s, 2H), 2.67 – 2.56 (m, 4H), 2.50 – 1.88 (m, 18H). **HRMS** (ESI): calc. for $C_{14}{}^{13}CH_{31}N_4O_4S^+$ [M+H]$^+$: 364.2094; found: 364.2096 *m/z*.

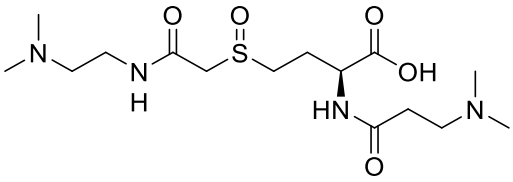

(2*S*)-4-(2-{[2-(Dimethylamino)ethyl]amino}-2-oxoethanesulfinyl)-2-[3-(dimethylamino)propanamido]-butanoic acid (9)

General procedure 7 (GP7): **8** (50 mg, 140 µmol, 1.0 equiv) was dissolved in 2 mL dest. H_2O. After the pH value was set to pH = 2 (HCl, 2M), mCPBA (31 mg, 140 µmol, 1.0 equiv) was added and the reaction mixture was stirred at rt for 20 min. The oxidation was monitored by LC-MS. After completion, residual mCPBA was removed by extraction with DCM (4 x 10 mL). Lyophilization of the aqueous phase gave **9** as a colourless solid (40 mg, 0.11 mmol, 75%).

^{1}H-NMR (400 MHz, D_2O) δ = 4.46 (td, *J* = 8.1, 5.1, 1H), 3.90 – 3.72 (m, 2H), 3.6 – 3.51 (m, 2H), 3.34 (td, *J* = 6.7, 1.8 Hz, 2H), 3.25 (t, *J* = 6.0 Hz, 2H), 3.06 – 2.85 (m, 2H), 2.82 (d, *J* = 9.5 Hz, 12H), 2.76 (t, *J* = 6.8 Hz, 2H), 2.34 – 2.19 (m, 1H), 2.17 – 2.04 (m, 1H) *ppm*. **^{13}C-NMR** (101 MHz, D_2O) δ = 174.4, 171.7, 166.9, 56.2, 56.0, 55.9, 53.3, 47.3, 47.2, 42.9, 42.8, 34.9, 29.5, 24.0 *ppm*. **HRMS** (ESI): calc. for $C_{15}H_{31}N_4O_5S^+$ $[M+H]^+$: 379.2010; found: 379.2012 *m/z*.

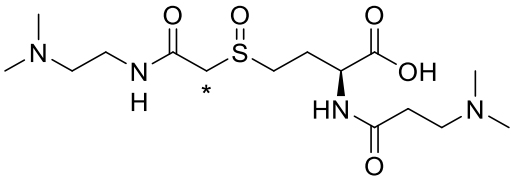

(2*S*)-4-[2-{[2-(Dimethylamino)ethyl]amino}-2-oxo(1-^{13}C)ethanesulfinyl]-2-[3-(dimethylamino)propanamido]-butanoic acid (9*)

Following **GP7**: **8*** (145 mg, 390 µmol, 1.0 equiv) furnished **9*** as a colourless solid (104 mg, 273 µmol, 70%).

^{1}H-NMR (400 MHz, D_2O) δ = 4.46 (ddt, *J* = 15.6, 10.1, 5.0 Hz, 1H), 4.10 – 3.50 (m, 4H), 3.35 (dt, *J* = 8.0, 4.0 Hz, 2H), 3.24 (t, *J* = 6.2 Hz, 2H), 3.07 – 2.95 (m, 2H), 2.82 (d, *J* = 9.4 Hz, 12H), 2.75 (q, *J* = 6.7 Hz, 2H), 2.29 (dp, *J* = 13.5, 7.4 Hz, 1H), 2.19 – 2.00 (m, 1H) *ppm*. **HRMS** (ESI): calc. for $C_{14}{}^{13}CH_{31}N_4O_5S^+$ $[M+H]^+$: 380.2043 found: 380.2045 *m/z*.

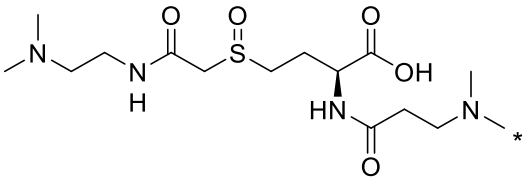

(2*S*)-4-(2-{[2-(Dimethylamino)ethyl]amino}-2-oxoethanesulfinyl)-2-(3-{methyl[(^{13}C)methyl]amino}propanamido)butanoic acid (9)**

Following **GP7**: **8**** (105 mg, 290 µmol, 1.0 equiv) furnished **9**** as a colourless solid (75 mg, 198 µmol, 69%).

^{1}H-NMR (400 MHz, D_2O) δ = 4.52 (dd, J = 8.7, 5.1 Hz, 1H), 3.71 – 3.29 (m, 8H), 3.10 – 2.62 (m, 16H), 2.50 – 2.17 (m, 2H) *ppm*. **HRMS** (ESI): calc. for $C_{14}{}^{13}CH_{31}N_4O_5S^+$ $[M+H]^+$: 380.2043; found: 380.2042 *m/z*.

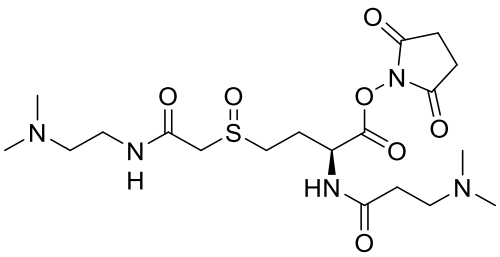

2,5-Dioxopyrrolidin-1-yl (2*S*)-4-[(2-{[2-(dimethylamino)ethyl]amino}-2-oxoethyl)sulfanyl]-2-[3-(dimethylamino)propanamido]butanoate (2)

General procedure 8 (GP8): Sulfoxide **9** (80 mg, 211 µmol, 1.0 equiv) was dissolved in 5 mL DMF. Then, dry pyridine (33 µg, 422 µmol, 2.0 equiv) and NHS-TFA (89 mg, 422 µmol, 2.0 equiv) were added to the reaction mixture. The reaction was monitored by LC-MS. After completion, the reaction mixture was concentrated *in vacuo.* The resulting orange oil was dissolved in acetonitrile and precipitated with cold acetone yielding **2** as a colourless solid (35 mg, 73.4 µmol, 35%).

HRMS (ESI): calc. for $C_{18}{}^{13}CH_{34}N_5O_7S^+$ $[M+H]^+$: 476.2174; found: 476.2173 *m/z*

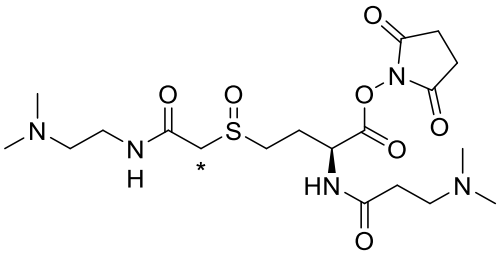

2,5-Dioxopyrrolidin-1-yl (2*S*)-4-{[2-{[2-(dimethylamino)ethyl]amino}-2-oxo(1-^{13}C)ethyl]sulfanyl}-2-[3-(dimethylamino)propanamido]butanoate (2*)

Following **GP8**: **9*** (50 mg, 132 µmol, 1.0 equiv) furnished **2*** as a colourless solid (20 mg, 42 µmol, 32%).

HRMS (ESI): calc. for $C_{18}{}^{13}CH_{34}N_5O_7S^+$ $[M+H]^+$: 477.2207; found: 477.2212 *m/z*.

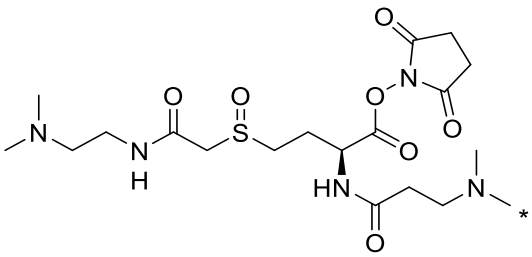

2,5-Dioxopyrrolidin-1-yl (2*S*)-4-[(2-{[2-(dimethylamino)ethyl]amino}-2-oxoethyl)sulfanyl]-2-(3-{methyl[(*^{13}C)methyl]amino}propanamido)butanoate (2)**

Following **GP8**: **9**** (75 mg, 198 µmol, 1.0 equiv) furnished **2**** as a colourless solid (30 mg, 63 µmol, 32%).

HRMS (ESI): calc. for $C_{18}{}^{13}CH_{34}N_5O_7S^+$ $[M+H]^+$: 477.2207; found: 477.2206 *m/z*.

IV. Mass spectrometric analysis

IV. Mass spectrometric analysis

Sample Preparation:

For the MS-experiments, *HEK293T* (ATCC-CRL-3216) lysate was used. After determining the protein content *via* Bradford-Assay, 150 µg of the lysate were solved in 200 µL digest-buffer (50 mM TEAB pH = 8.5, 1 mM $MgCl_2$), the disulfide bonds of proteins were reduced with DTT (final concentration 20 mM, 60 °C, 1 h) and cysteines were alkylated using iodacetamide (final concentration 40 mM, room temperature, 30 min, dark). After adjusting the pH of the samples to 7-8 using 1 mM TEAB, 3 µg Trypsin (MS-grade, *Pierce, Thermo Fisher Scientific*) in 6 µL 50 mM AcOH was added and the sample was digested for 2 h at 55 °C. Afterwards, the peptides were desalted and concentrated using Stage-Tips.[5]

40 µg of lyophilized lysate was solved in 40 µL of TEAB-buffer (150 mM, pH = 8.5). Four portions of 8.5 µL (8.50 µg protein content) each were divided and labelled with TMT-126, TMT-127, SOT-179 and SOT-180, respectively.

For TMT-labelling, the instructions provided by the manufacturer were used *(Thermo Fisher Scientific*). In case of the SOT-reagents, a solution of SOT-179 and SOT-180 in dry DMSO with a concentration of 0.1 mg/µL was used for the labelling. The peptide mixture was diluted with 31.5 µL of TEAB-buffer (150 mM, pH = 8.5) and 1.5 mg of SOT-179 or SOT-180, respectively, in 15 µL DMSO was added. The samples were incubated for 1 h at room temperature. To quench residual reagent activity, 5 µL of a hydroxylamine-solution (5%) was added to each sample (15 min, rt).

The labelled lysates were combined in a 1 to 1 ratio, diluted with 1% $TFA_{(aq)}$ until an acidic pH was measured and then purified by Stage-Tips. For both the TMT- and the SOT-duplexes, the complete sample consisted of 1.1 µg of lysate protein content. Per measurement, in total 1 µg of lysate was injected for analysis.

To investigate the ratio distortion effect, Trypsin-digested BSA MS Standard (*NEB*) was also labelled with TMT or SOT according to the procedure above. HEK-lysates were labelled as described above for SOT and TMT and combined to give a human

peptide background in a labelled ratio of 1 to 1. Into this background, the labelled BSA was added in a ratio of 4 to 1. The peptides were purified by Stage-Tips. Per measurement a total of 1 µg labelled *HEK*-background lysate and 0.15 pmol of labelled BSA-peptides were injected for analysis to acquire data which show a high ratio distortion effect.

Mass Spectrometric analysis:

The samples were analyzed with an UltiMate 3000 RSLCnano liquid chromatography system (*Dionex, Thermo Fisher Scientific*) attached to a Q Exactive HF mass spectrometer (*Thermo Fisher Scientific*). They were concentrated on a µ-precolumn cartridge (PepMap100, C_{18}, 5 µM, 100 Å, size 300 µm i.d. x 5 mm (*Dionex, Thermo Fisher Scientific*)) and further processed on a in house packed analytical column (ReproSil-Pur 120 C18-AQ, C_{18}, 1.9 µM, 120 Å (*Dr. A Maisch GmbH*), packed into a 75 µm i.d. x 150 mm fused silica picotip emitter with an 8 µm tip (*New Objective*).

The samples were processed *via* a 120 min multi-step analytical separation at a flow rate of 300 nL/min and a column temperature of 30 °C. Only LC-MS grade solvents were used (solvent A: water + 0.1% formic acid; solvent B: acetonitrile + 0.1% formic acid). The gradient with percentages of solvent B was programmed in the following way:

1% for 3.5 minutes; from 1% to 8% in 1.5 minutes; from 8% to 32% in 95 minutes; from 32% to 60% in 5 minutes; from 60% to 85% in 5 minutes; 85% for 2 minutes; from 85% to 1% in 3 minutes; 1% for 5 minutes.

Mass spectrometric analysis of the *HEK*-lysates was done with a full mass scan in the mass range between m/z 300 and 1750 at a resolution of 120k, an AGC target of 3e6 charges and a maximum ion injection time of 20 ms in profile mode. Following this survey scan, the 15 most intense ions were selected, fragmented and measured in profile mode with the following parameters: resolution of 30000; AGC target of 1e5 charges; maximum ion injection time of 100 ms; isolation window of 1.4 m/z; fixed first mass of 115 m/z; normalized HCD energy of 28%. Signals with an unrecognized charge state or a charge state of 1, 7, 8 or higher weren't picked for fragmentation. To reduce supersampling of the peptides, signals were excluded from the analysis for 20 s after being selected for isolation and fragmentation. The peptide match setting was set to "-" and the exclude isotope setting was set to "on".

In case of the distorted BSA-*spike-in* samples, the same gradient was chosen, but the normalized HCD-energy was set to 30%. All other acquisition parameters remained unchanged.

Data Analysis:

Protein and peptide identification was done using the MaxQuant software version 1.6.0.16.[6] A reporter ion MS2-analysis was chosen. As isobaric label modifications, either the supplied TMT-labels or the SOT-reagents designed by this study were chosen. The intact modification mass of the isobaric SOTs is 361.18648 Da and modification can occur on the peptide N-terminus and lysine residues. For the reporter ion masses, 178.07760 Da for SOT-179 and 179.08095 Da for SOT-180 was set as the neutral mass. Reporter mass tolerance was set to 0.003 Da. Trypsin was set as the used protease and up to two missed cleavages were allowed. Carbamidomethylation was set as static modification on cysteine residues. Oxidation of methionines was set as variable modification. In the first search, 20 ppm and in the main search, 4.5 ppm peptide mass deviation was allowed. As database, a .FASTA-file from Uniprot of *homo sapiens* (Uniprot Proteome ID: UP000005640) downloaded on the 29.08.2017 was used. For analysis of the BSA *spike-in* samples, a different .FASTA was used in which the bovine serum albumin (Uniprot: P02769) sequence was inserted at the beginning. Minimum peptide length was set to 7. PSM and protein FDRs were set to 0.01. For the BSA *spike-in* samples only, the often included search for common contaminants was omitted, since BSA is also contained in this contaminants .FASTA-file.

For further analysis of the acquired data, RawMeat V2.0 build1007 (*VAST Scientific*) was utilized to determine the precursor charge state distribution. If necessary, the .raw file format was converted to .mzXML using the Proteom Wizard MSConvert application. The Peak picking was set to use the vendors peak picking algorithm, centroiding the peaks from MS1 and MS2-scans.

To gain further insight into the fragmentation behavior of the new designed reagent, a novel software pipeline was created. The Java 1.8 code consists of tools to automatically calculate the different m/z-values associated with modified and unmodified peptide fragment ions, determine their sum formula, comparing the peaks from measured spectra to the calculated data and to give out tables identifying the

detected fragments. A schematic representation of the workflow is shown in **Fehler! Verweisquelle konnte nicht gefunden werden.**. The software is freely available. For the software package and instructions how it is used, contact the authors of the paper.

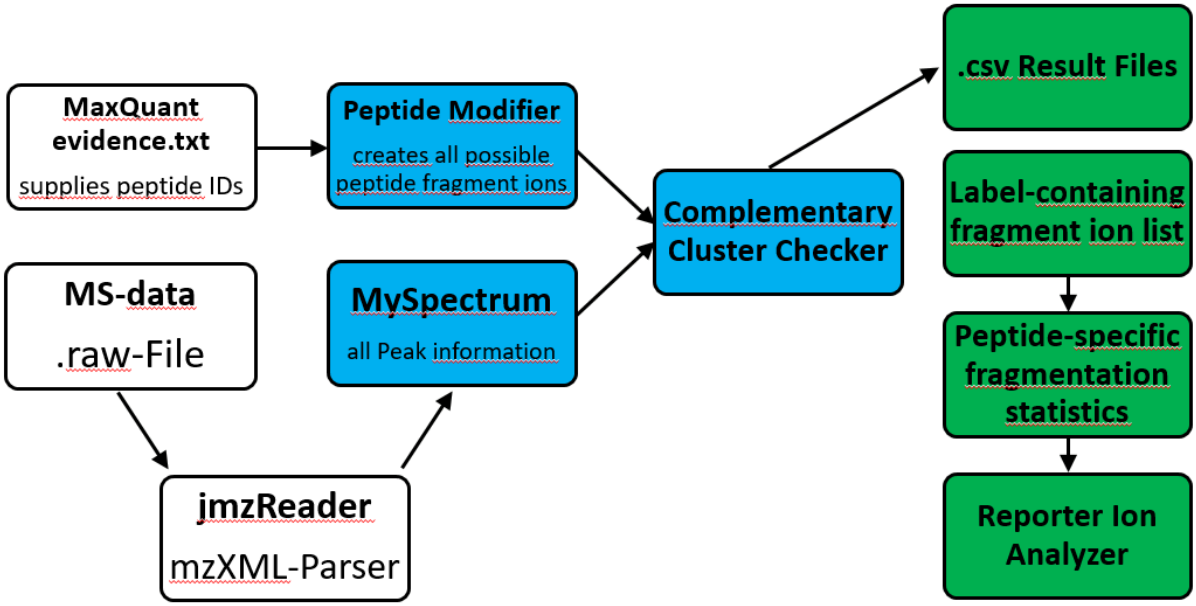

Supplementary Figure 1: Automated Data analysis pipeline.

To achieve this, .raw-Files containing the complete MS-data were first converted to .mzXML-files as described above. Next, the *mzXML-parser* node from the Java MS-data parser library *jmzReader* (*Griss et al.)* was utilized to read the generated .mzXML-files and to obtain the peak properties of interest (m/z-value, intensity).[7] Peptide identifications were then read from the *"evidence.txt"*-file generated by MaxQuant. Specifically, the peptide sequence, modifications on the precursor and the scan number were read from the MaxQuant evidence-file. Subsequently, the code generates the respective peptide and the corresponding *b*- and *y*-ions for the charge states z = 1 and z = 2, which are modified with the different combinations of intact label and the cleaved fragments forming the complementary ions. At the same time, the peak information of the MS^2-scan responsible for the identification is extracted by the *mzXML-parser* and an additional module. Next, for each possible modified *b*- and *y*-ion containing the intact or cleaved reagent, the respective spectrum is checked for the corresponding peak. To ensure the stringency of the mass comparison, only 5 ppm of mass deviation are allowed. Finally, hits are stored and given out at the end of the analysis as a .csv-file, where the hits can be sorted whether they contain cleaved or intact labels as modifications.

To even further analyze the data, another node takes all the matched fragments from the first result file and summarizes the fragment numbers for each individual peptide species. In addition, information about the reporter ion intensities can be read out from the MS-files to obtain the median reporter ion intensities.

Ratio calculation:

Although the quantification approach using the complementary ion clusters benefits from a huge reduction of ratio distortion effects and therefore improves the quantification accuracy significantly, the MS-signals must be processed further to give the relative ratios of the samples. Unlike in the reporter ion quantification approach, in which the (possible distorted) ratios can be readout directly from the reporter ion intensities after application of fixed isotopic purity correction factors, this is not the case when analyzing complementary ion clusters. Here, the naturally occurring isotope distribution prohibits the direct determination of the mixing ratios, because the isotope pattern of the light complementary ion and the signal arising from the heavier complementary ion overlap. Since the isotope pattern is not only dependent on the balancer-part of the complementary ion, but also on the residual peptide fragment composition, the influence of the isotope pattern must be calculated for every complementary ion cluster analyzed.

Hence, to approximatively determine the ratio between the light and heavy complementary ions, the abundance of the isotopic signal containing one additional neutron in relation to the monoisotopic signal of the light complementary ion must be calculated. Afterwards, this intensity must be subtracted from the heavy complementary ion signal to remove the isotope pattern interference (with the approximation that the isotope patterns of the light and heavy complementary ions are roughly the same). In addition, the balancer part of the heavy complementary ion SOT179^{c} contains a ^{13}C-atom as a heavy stable isotope marker. Since the commercial available ^{13}C-formaldehyde utilized during the synthesis of SOT179 contains also traces of ^{12}C-formaldehyde, this isotopic impurity leads to an increase in the light complementary ion signal. Fortunately, this isotopic impurity is very small (<0.4%) and can be determined by mass spectrometric analysis of the SOT179-balancer part. In Supplementary Figure , the contributions of the isotope pattern and the isotopic impurity towards the light and heavy complementary ion signals is visualized.

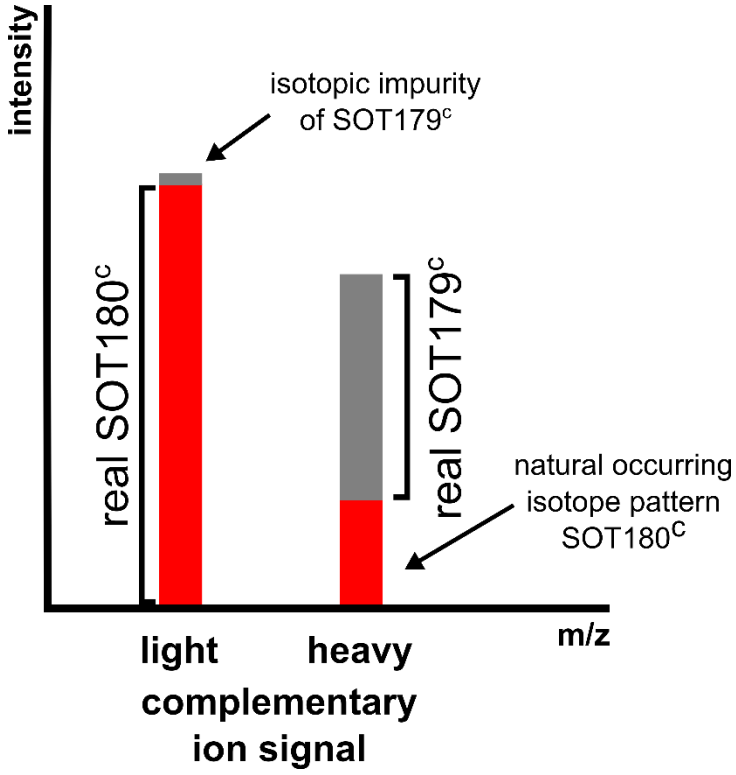

Supplementary Figure 2: Contributions towards the light and heavy complementary ion signal. While the natural occurring isotope pattern of SOT180^{c} leads to an increase in the heavy complementary ion signal, the isotopic impurities present in the balancer part of SOT179^{c} increase the light complementary ion signal.

For the calculation of the relative ratios, the isotopic impurity factor *x* is measured as the ratio of SOT179^{c}-signal intensity containing only ^{12}C-atoms divided by the SOT179^{c} signal intensity in which the desired ^{13}C-atom was incorporated (Eq. 1).

$$x = \frac{I\left(SOT179^{c}\left(^{12}C\right)\right)}{I\left(SOT179^{c}\left(^{13}C\right)\right)} \qquad (1)$$

Additionally, the isotope pattern factor λ is calculated from the sum formula of the light complementary ion, which is composed of the balancer and the identified peptide fragment part. The factor determines the relative intensity of the first isotopic signal (monoisotopic signal + one additional neutron n) in relation to the monoisotopic signal of SOT180^{c} (Eq. 2). It takes into account the natural abundances of heavy isotopes reported from the “Comission on Isotopic Abundances and Atomic Weights” of the IUPAC.[8]

$$\lambda = \frac{I(SOT180^{c}(n+1))}{I(SOT180^{c}(n))} \qquad (2)$$

Together with those parameters as well as the measured intensities of the light (I_l) and heavy (I_h) complementary ion signals, one can calculate the real intensities of the complementary ions I(SOT180$^c_{real}$) and I(SOT179$^c_{real}$) (Eqs. 3 and 4).

$$I_{SOT180^c_{real}} = I_l - \left(x \cdot I_{SOT179^c_{real}}\right) \quad (3)$$

$$I_{SOT179^c_{real}} = I_h - \left(\lambda \cdot I_{SOT180^c_{real}}\right) \quad (4)$$

By combining equations (3) and (4), the following equations arise to calculate the deconvoluted intensities of the complementary ion cluster (Eqs. 5 and 6).

$$I_{SOT180^c_{real}} = \frac{I_l - x \cdot I_h}{1 - x \cdot \lambda} \quad (5)$$

$$I_{SOT179^c_{real}} = \frac{I_h - \lambda \cdot I_l}{1 - x \cdot \lambda} \quad (6)$$

For each identified complementary ion cluster pair, the calculation is done by the Java application, and the ratio is reported in a .csv-File. Since there are only two possible y1-ions in the sample (in case of trypsin as the used protease, R and K), the y1-complementary ion cluster could still be subject to ratio distortion. Therefore, y1-complementary ion clusters are removed from the analysis to avoid the reintroduction of ratio distortion. For the quantification experiments, the background-protein median ratio was normalized to 1.

V. Additional Figures

A. SOT - Duplex

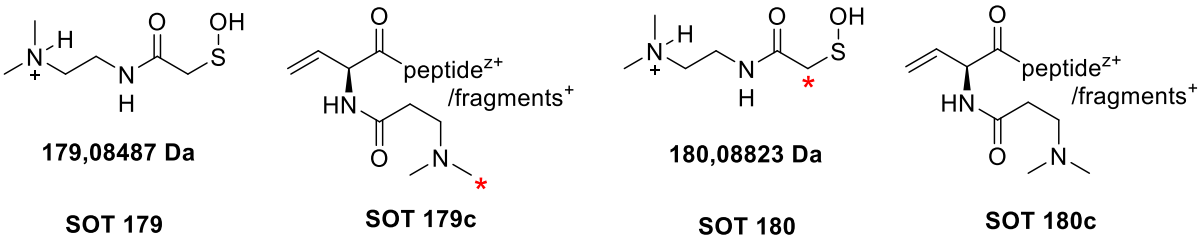

SOT 179 **SOT 179c** **SOT 180** **SOT 180c**

B. SOT - Nineplex Reagents (SOT^{9})

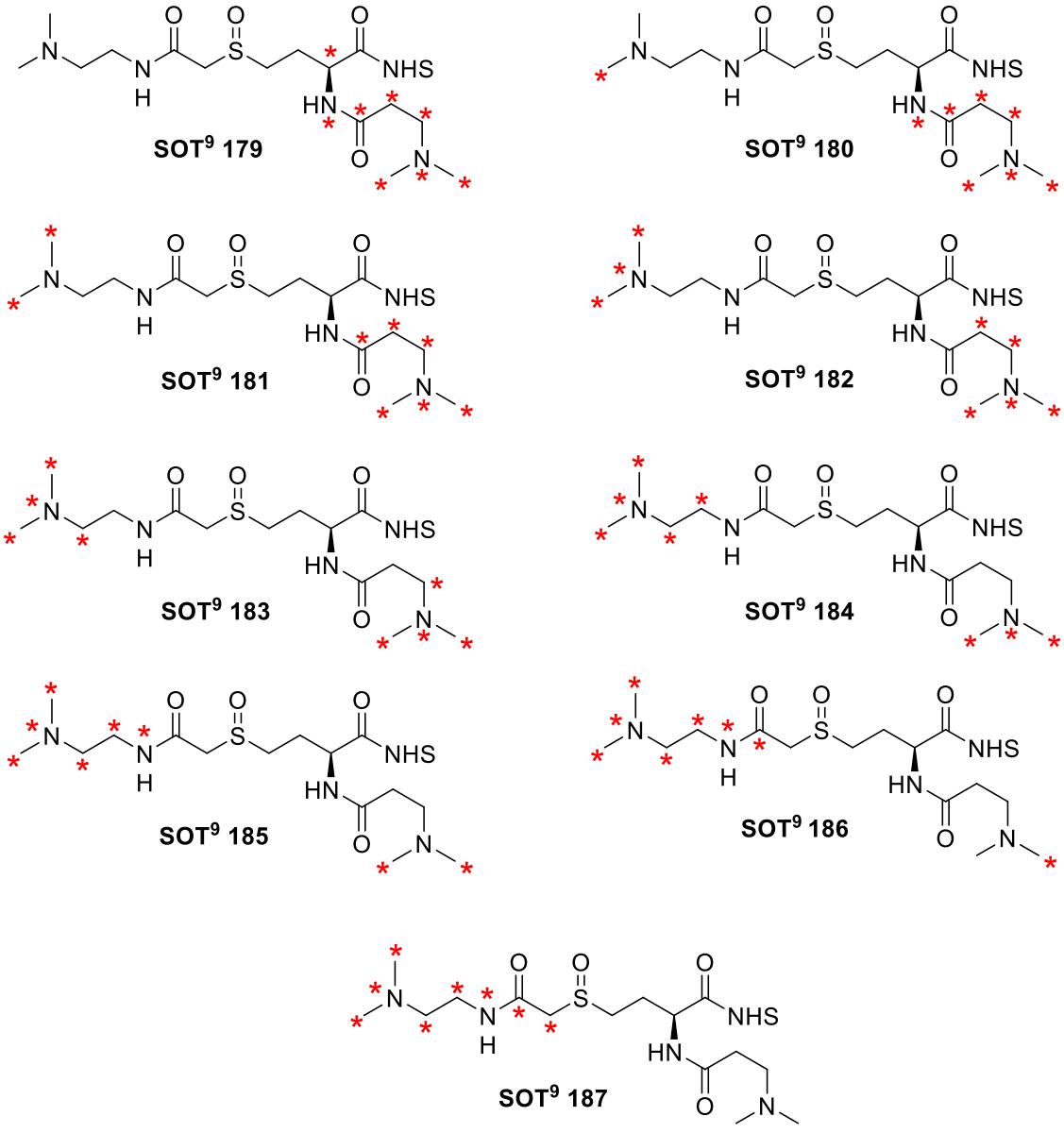

Supplementary Figure 3: A) Fragmentation behavior of the SOT duplex reagents. B) Proposed structures of the SOT-Nineplex reagent (SOT^{9}). Asteriks positions indiciate the presence of heavy isotopolouges (^{13}C, ^{15}N).

VI. NMR spectra

Benzyl bromo(2-^{13}C)acetate (11)

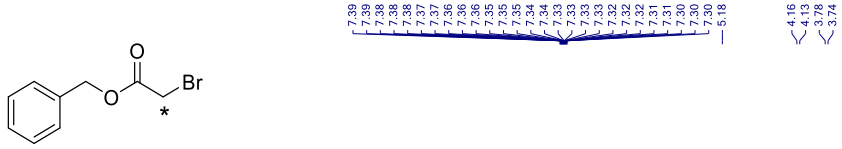

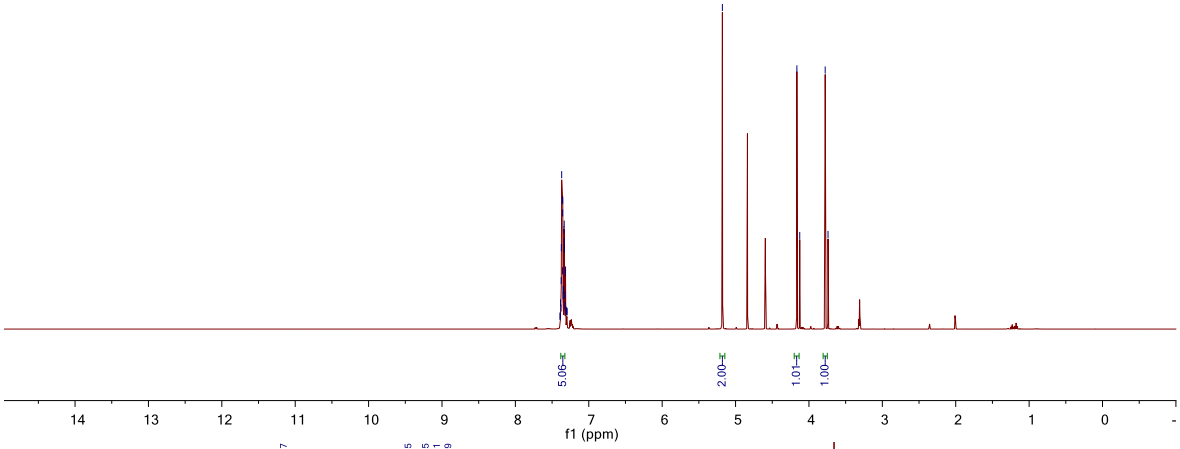

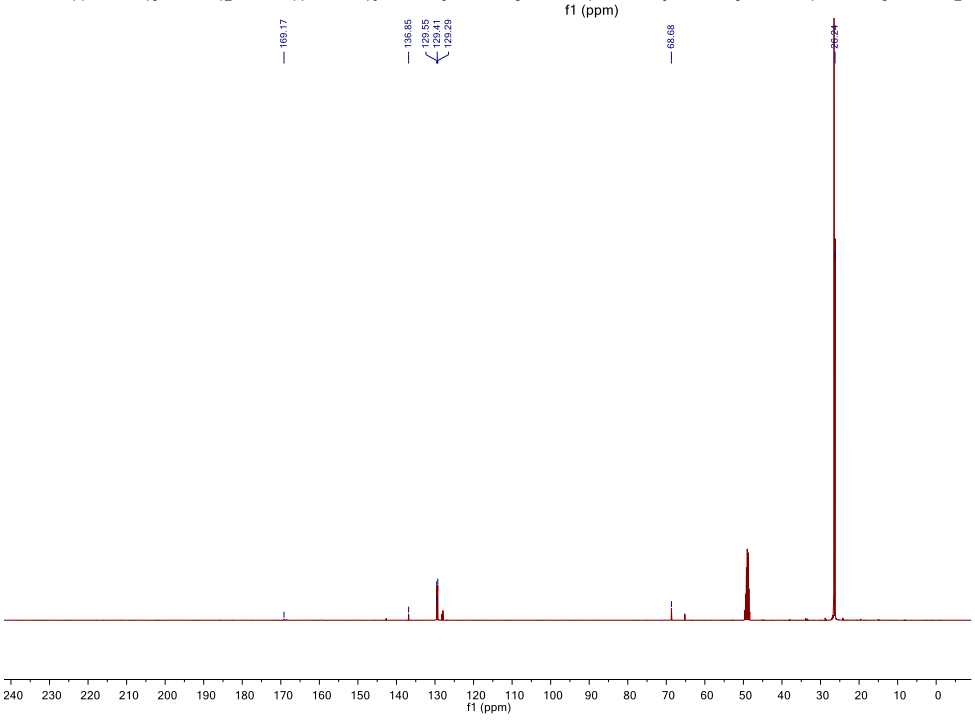

Methyl 3-[benzyl(methyl)amino]propanoate (13)

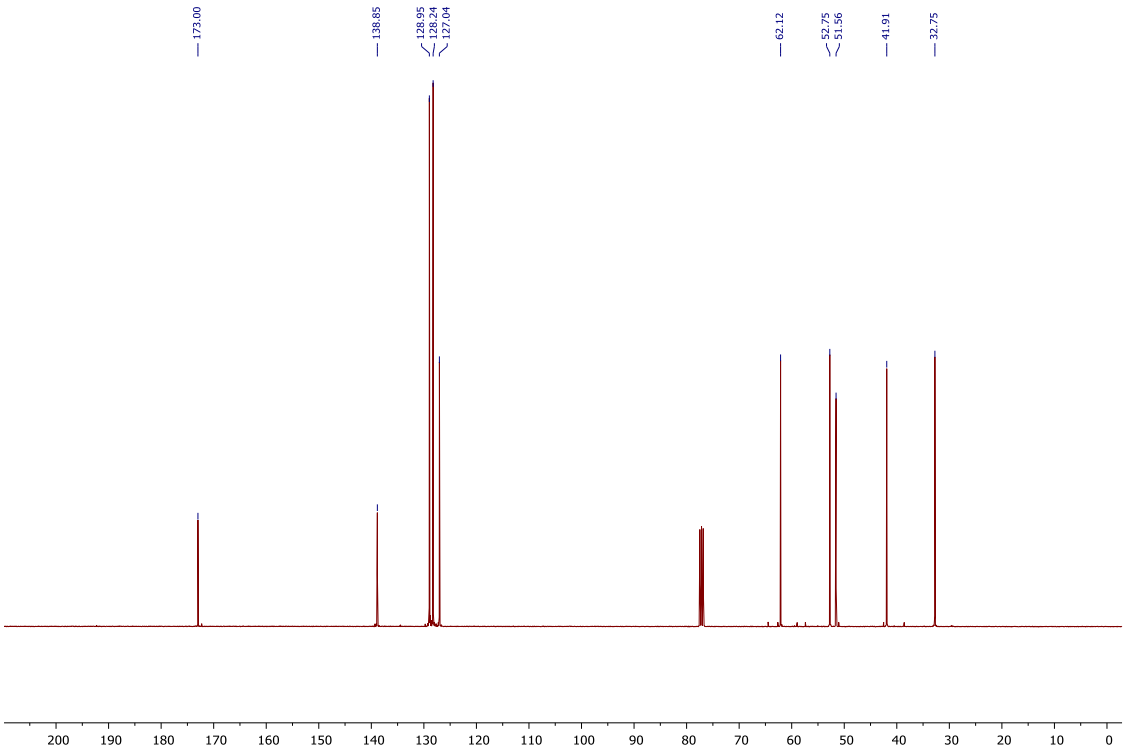

3-(Methylamino)propanoic acid hydrochloride (14)

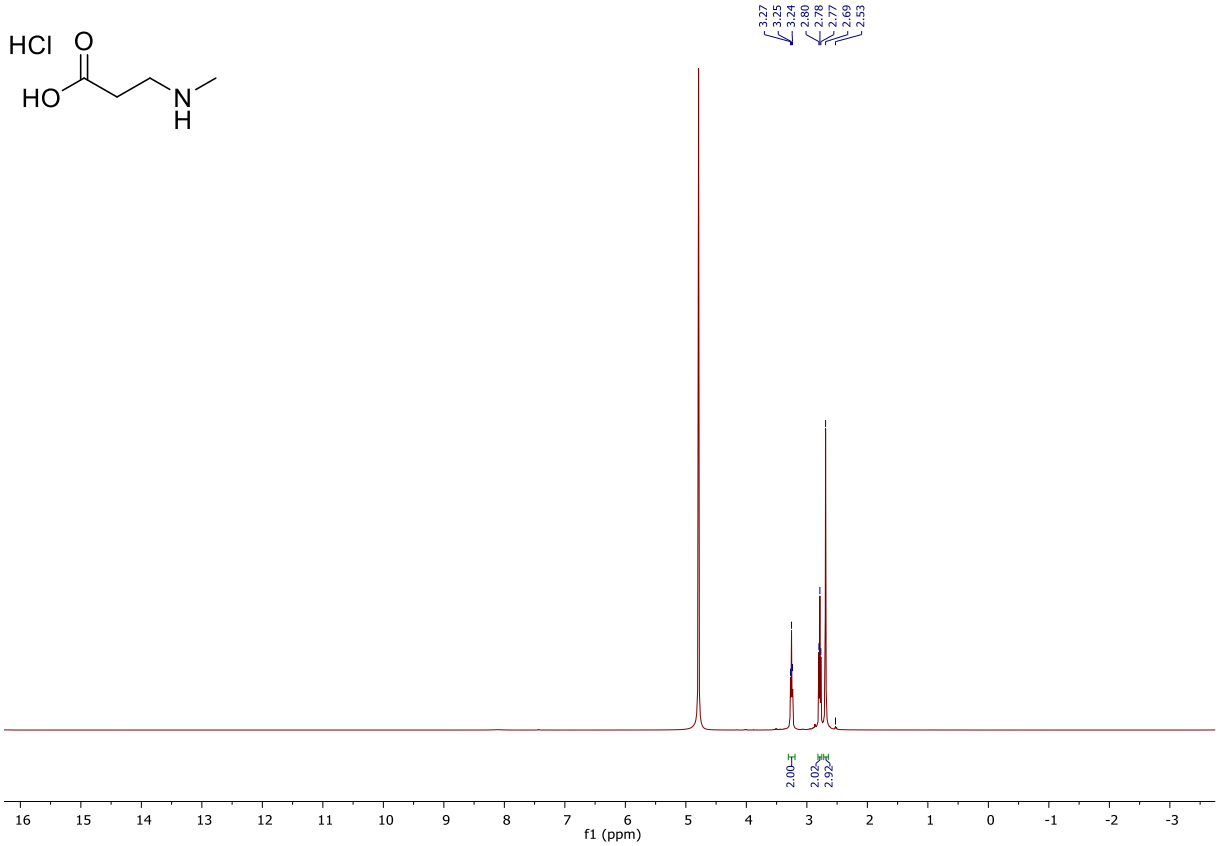

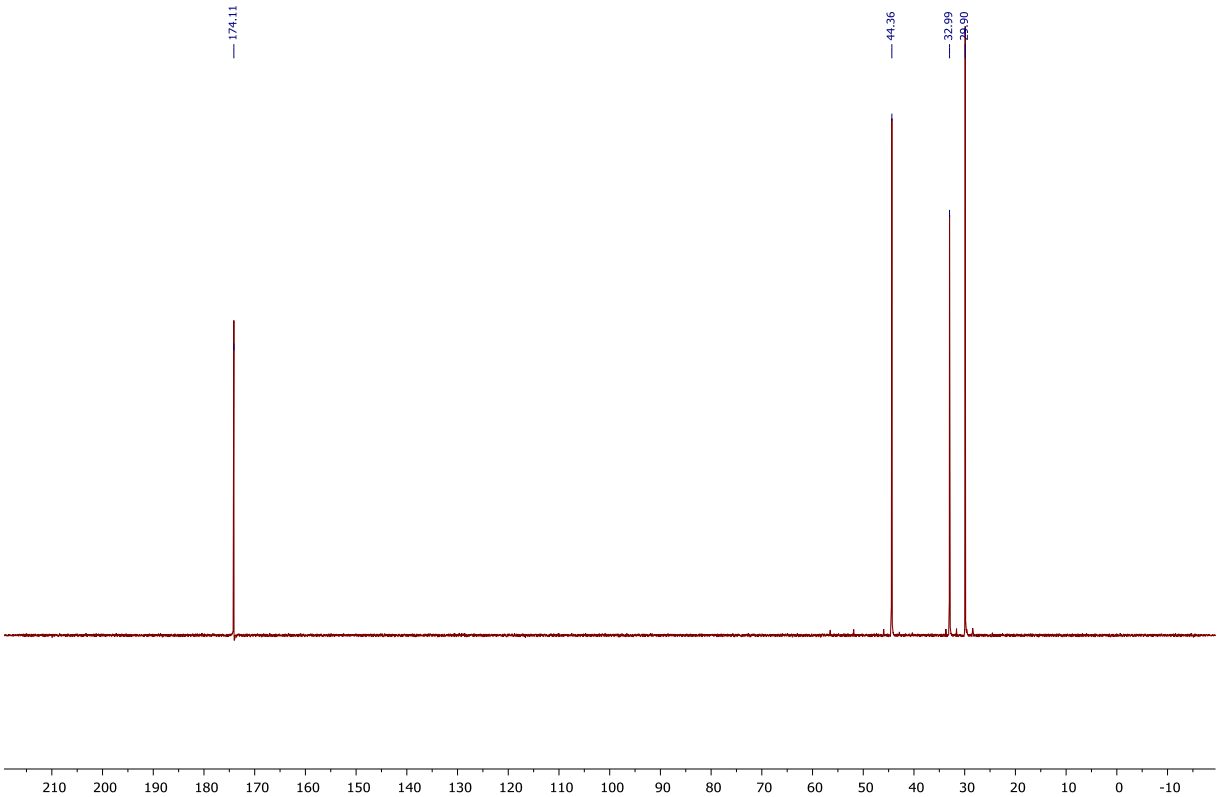

3-{Methyl[(^{13}C)methyl]amino}propanoic acid hydrochloride (10)

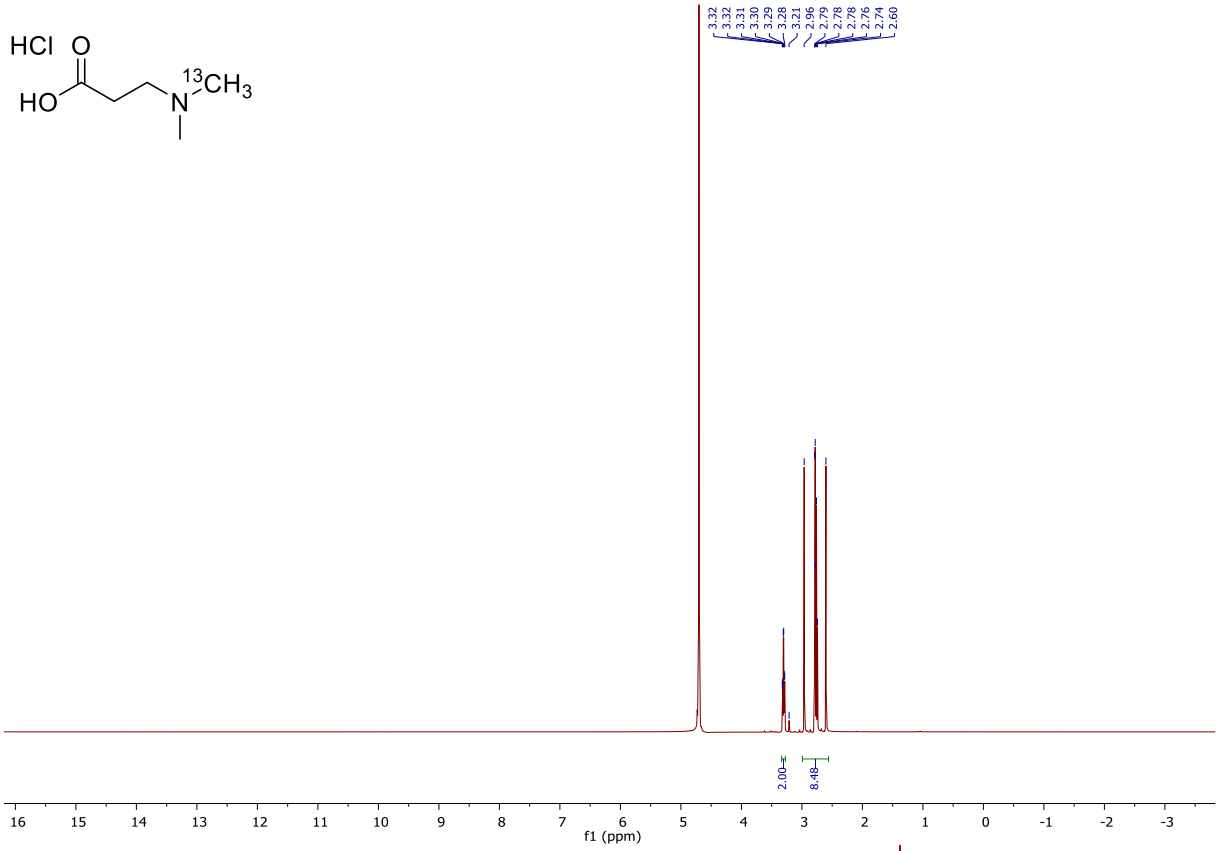

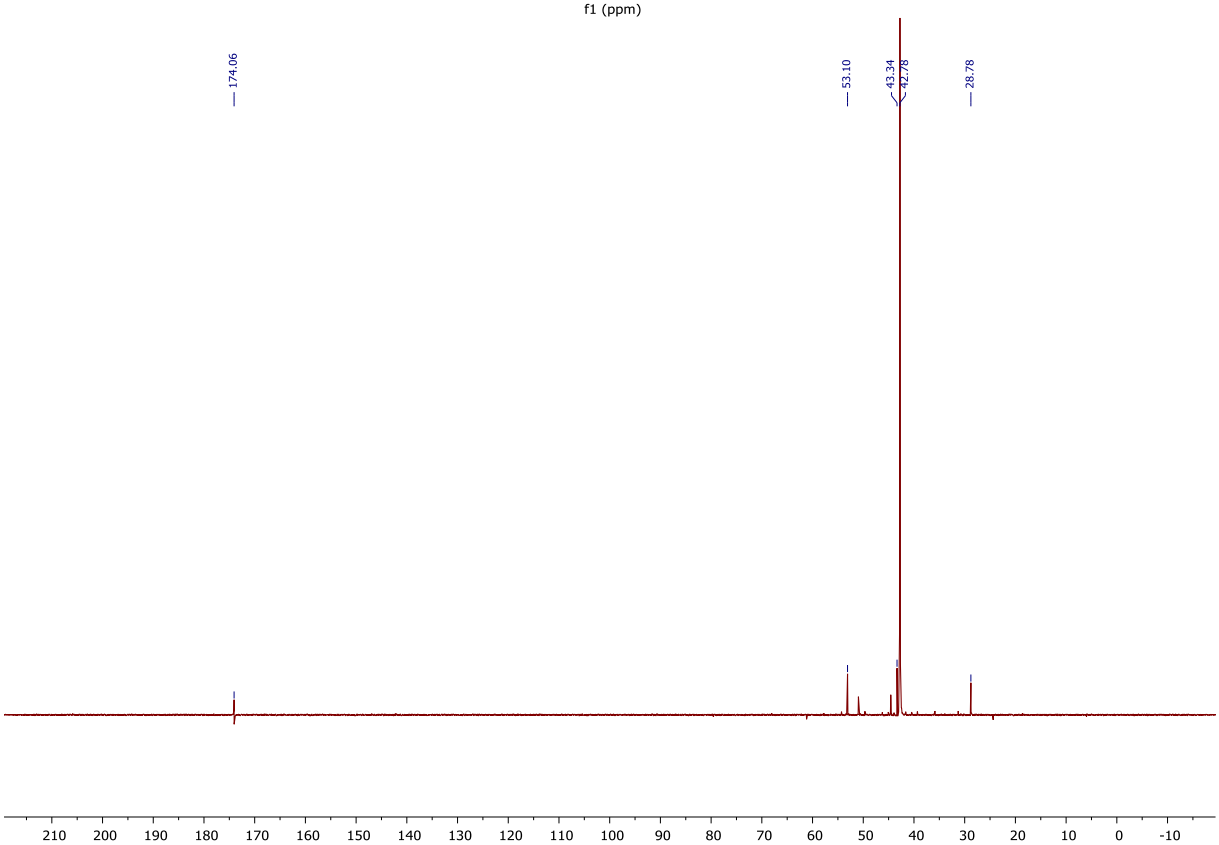

Methyl (2*R*)-2-amino-4-{[(3*S*)-3-amino-4-methoxy-4-oxobutyl]disulfanyl}butanoate (3)

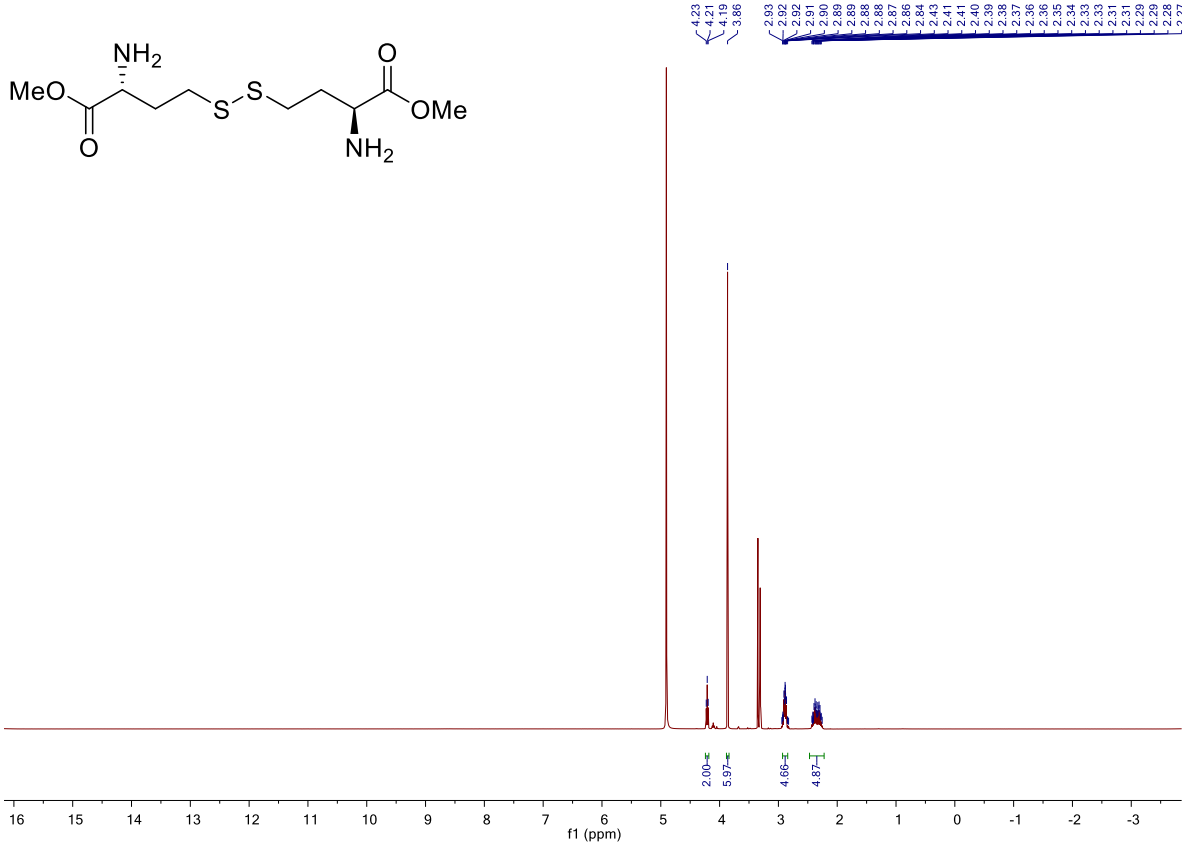

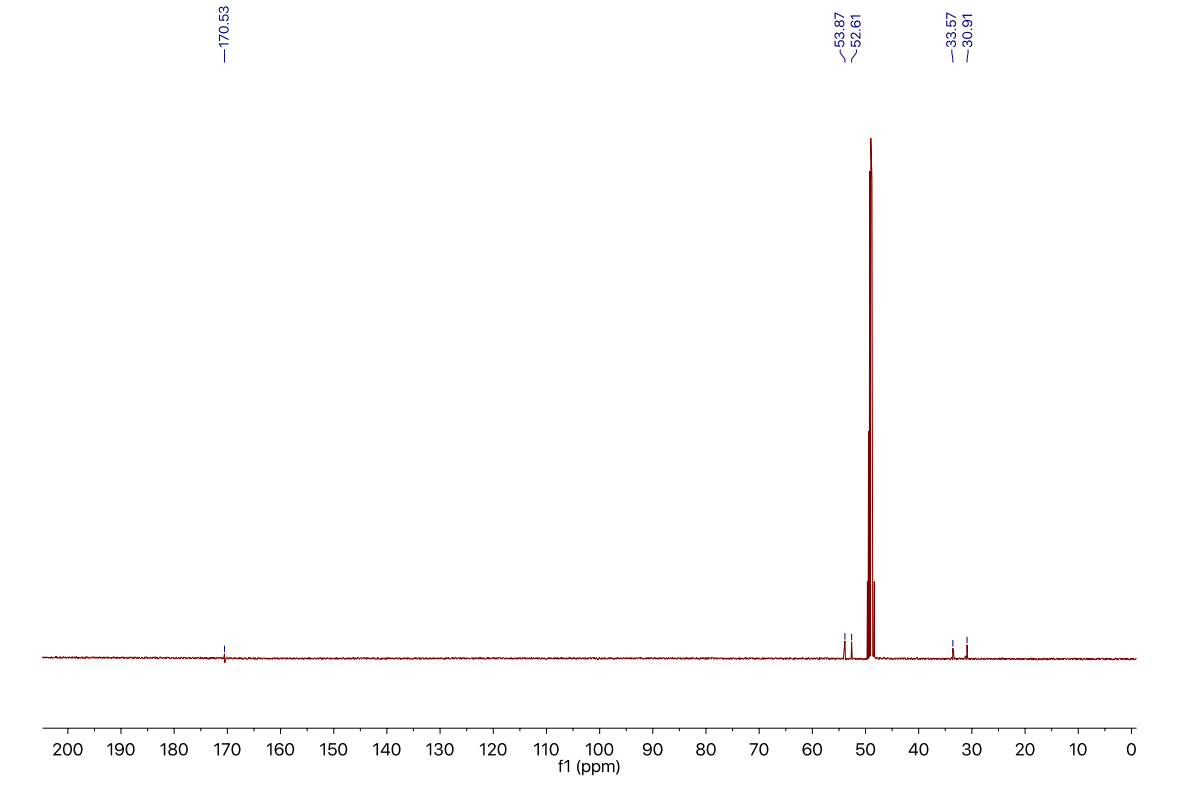

Methyl (2*R*)-2-[3-(dimethylamino)propanamido]-4-({(3*S*)-3-[3-(dimethylamino)propanamido]-4-methoxy-4-oxobutyl}disulfanyl)butanoate (4)

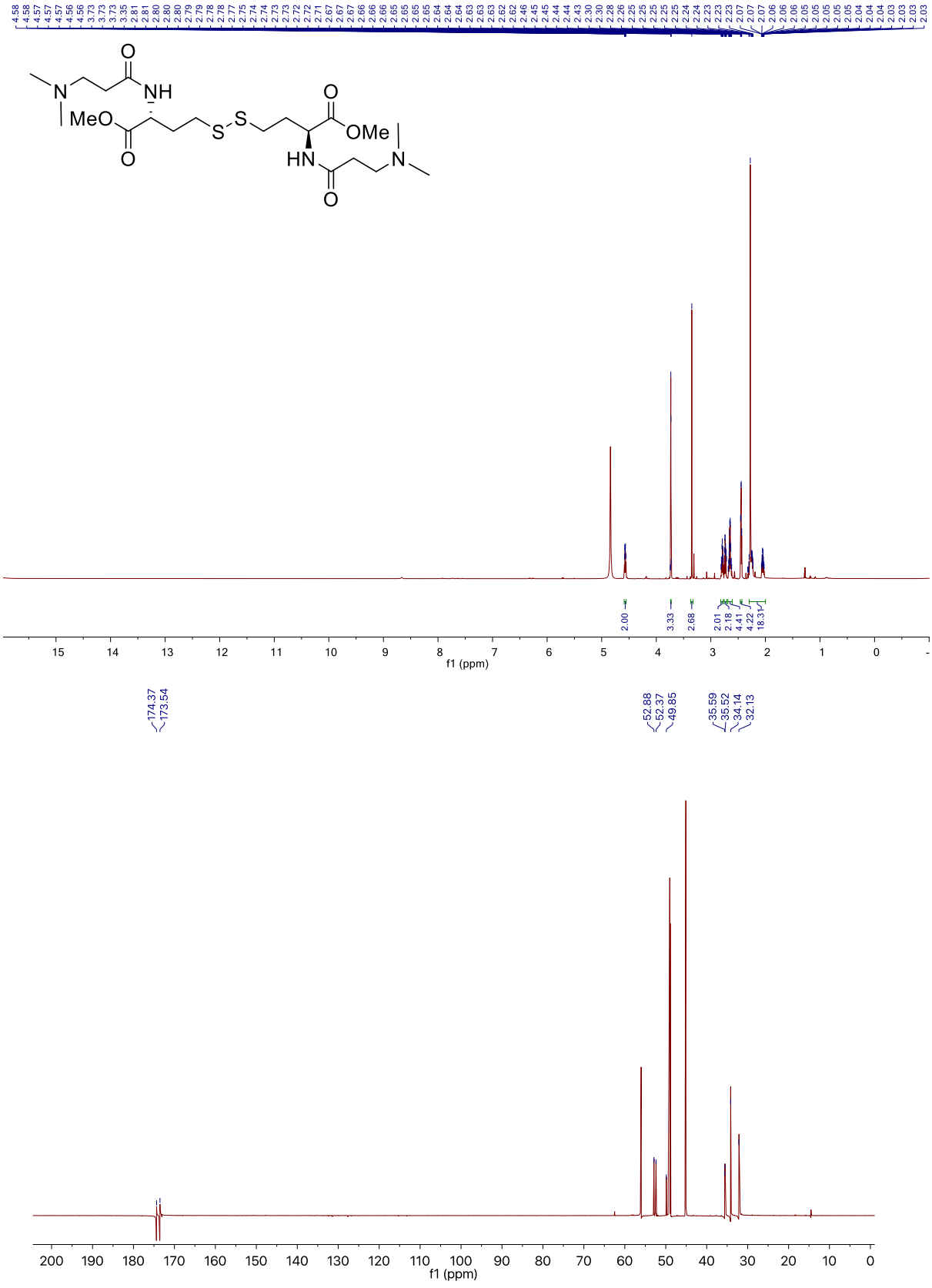

Dimethyl-4,4'-disulfanediyl(2R,2'S)-bis(2-(3-(methyl(methyl-13C)amino)-propanamido)-butanoate) (4)**

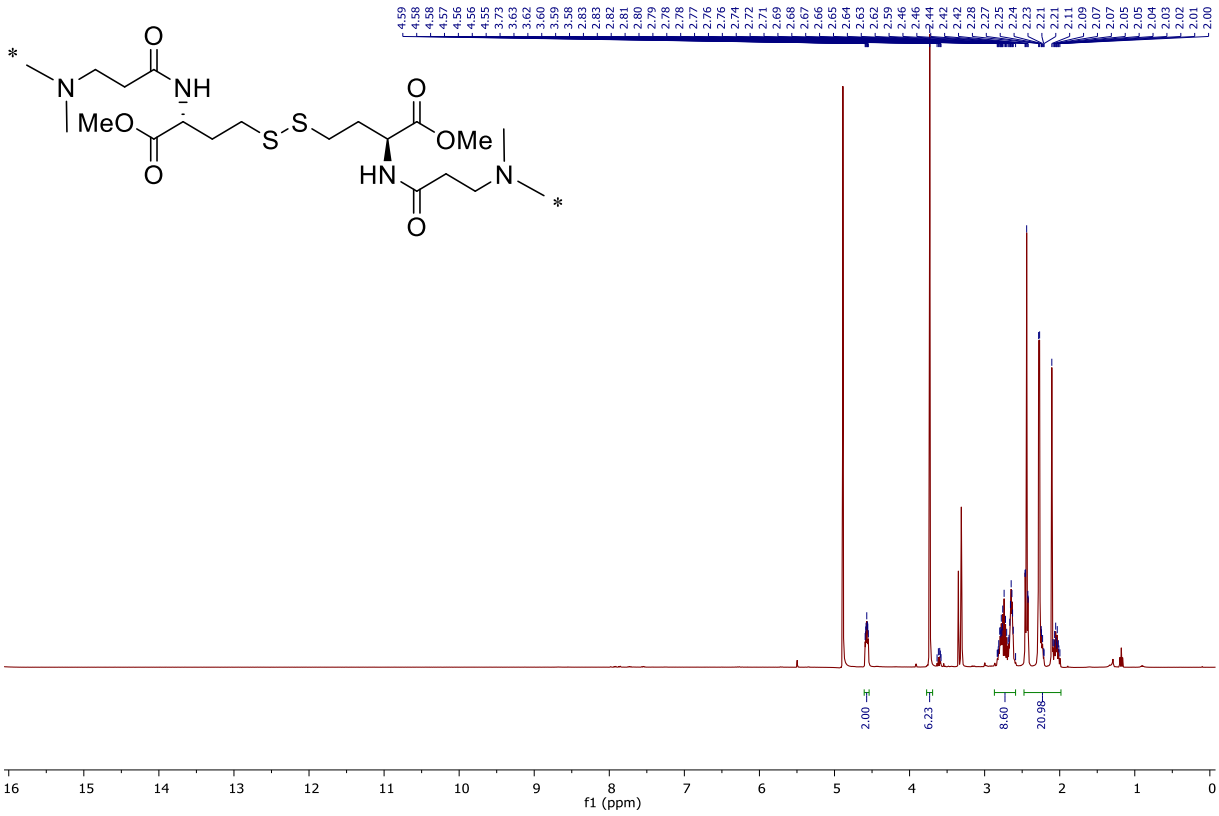

Methyl (2*S*)-4-{[2-(benzyloxy)-2-oxoethyl]sulfanyl}-2-[3-(dimethylamino)propanamido]butanoate (5)

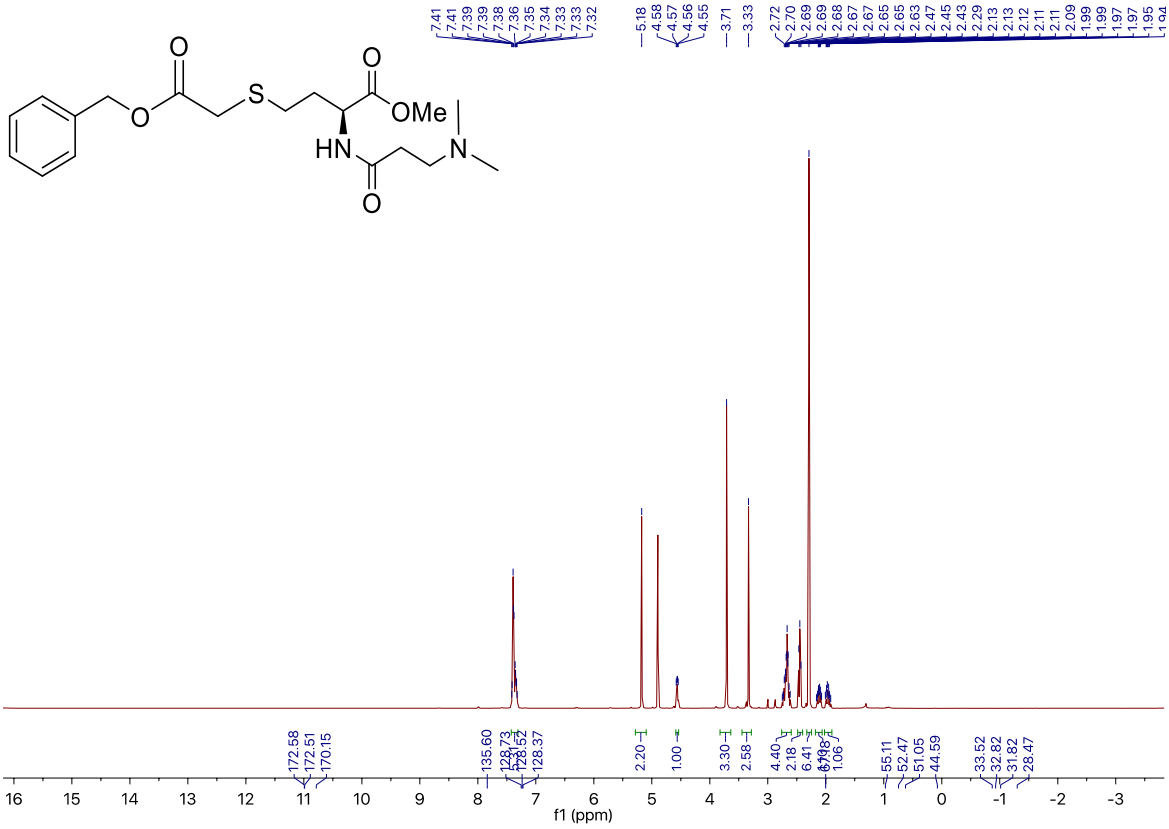

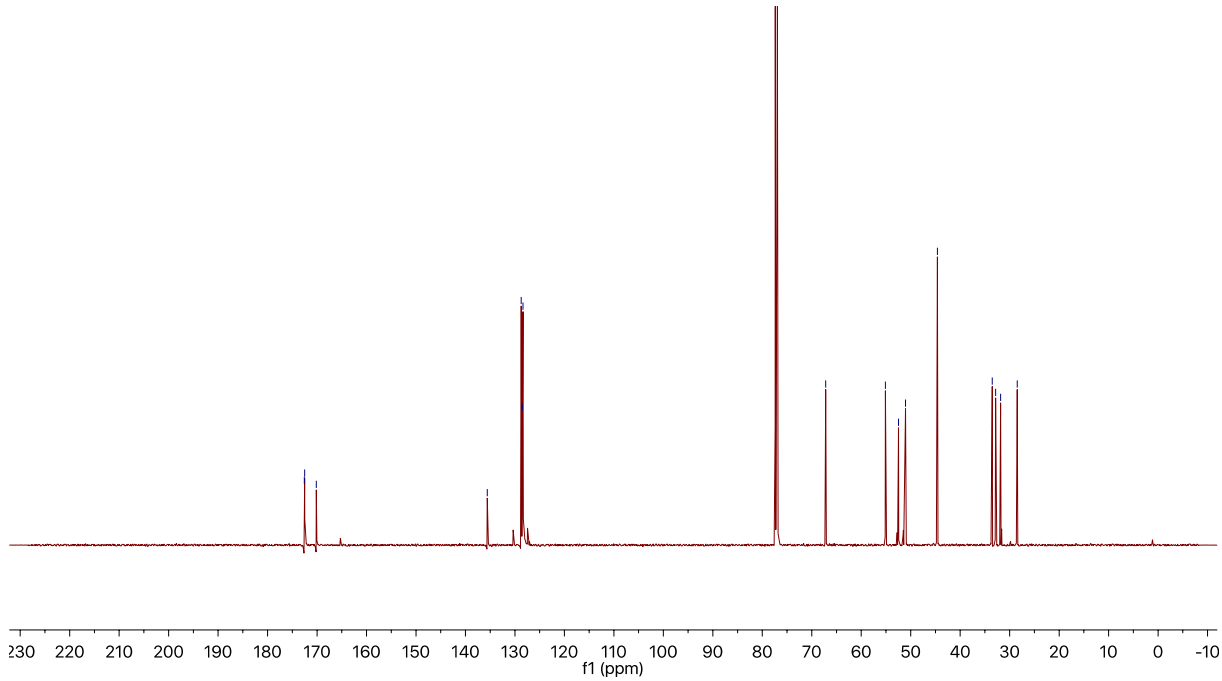

Methyl (2S)-4-{[2-(benzyloxy)-2-oxo(1-13C)ethyl]sulfanyl}-2-[3-(dimethylamino)propanamido]butanoate (5*)

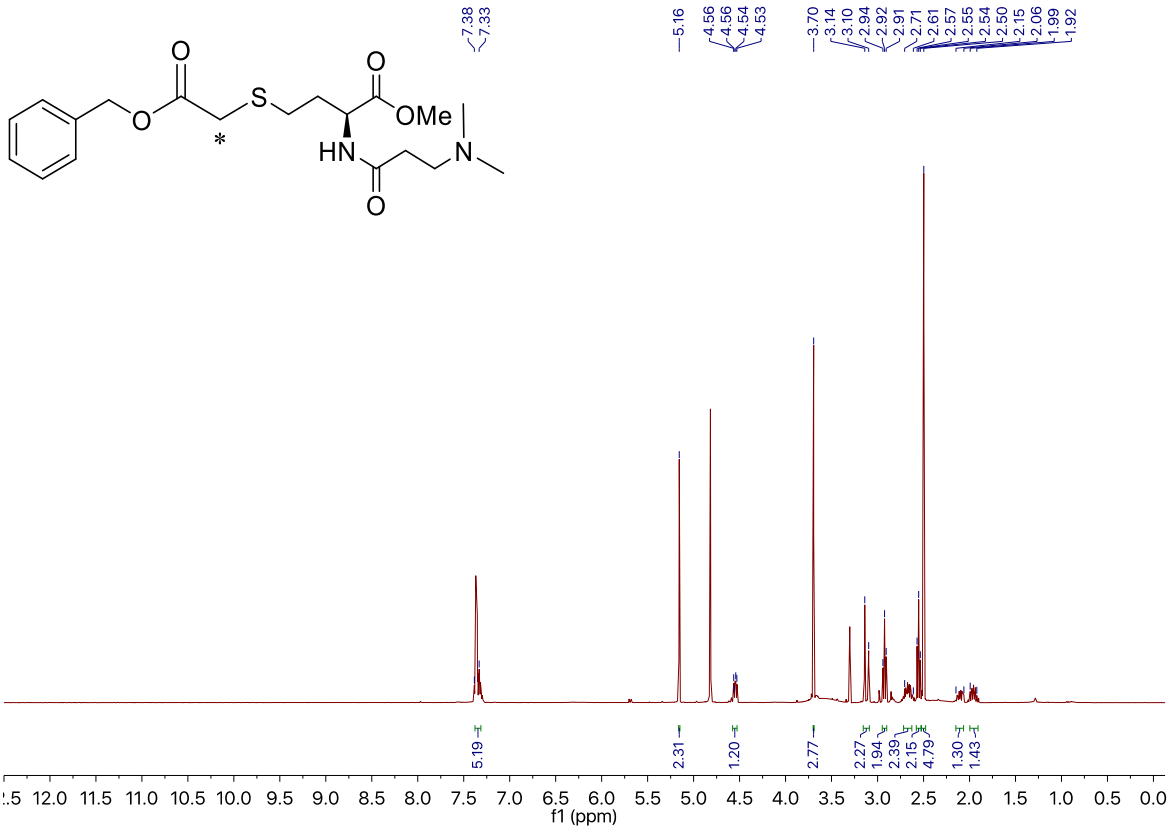

Methyl (2*S*)-4-{[2-(benzyloxy)-2-oxoethyl]sulfanyl}-2-(3-{methyl[(^{13}C)methyl]amino}propanamido)butanoate (5)**

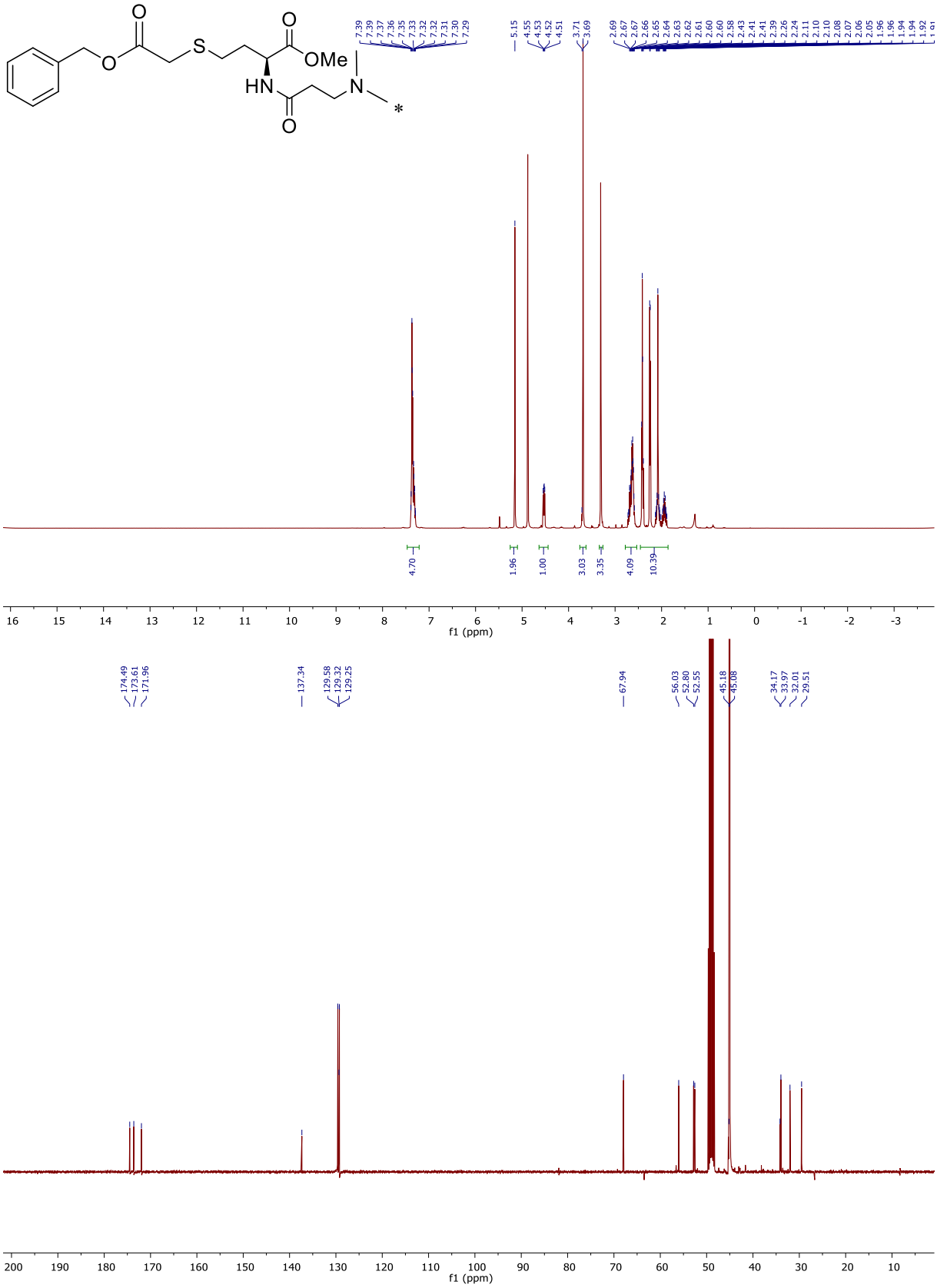

({(3*S*)-3-[3-(Dimethylamino)propanamido]-4-methoxy-4-oxobutyl}sulfanyl)acetic acid (6)

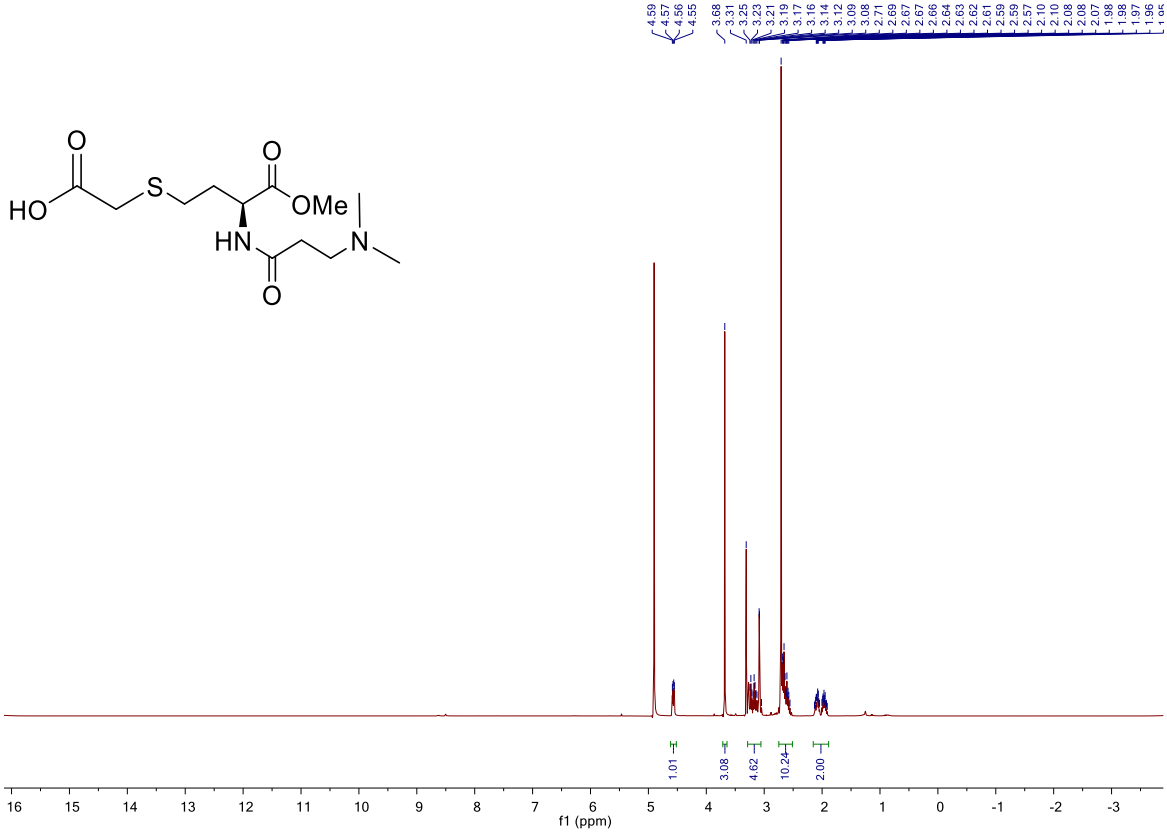

({(3S)-3-[3-(Dimethylamino)propanamido]-4-methoxy-4-oxobutyl}sulfanyl)(2-13C)acetic acid (6*)

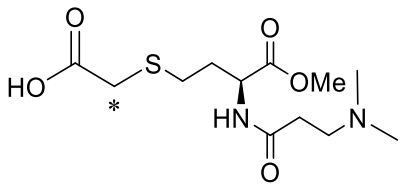

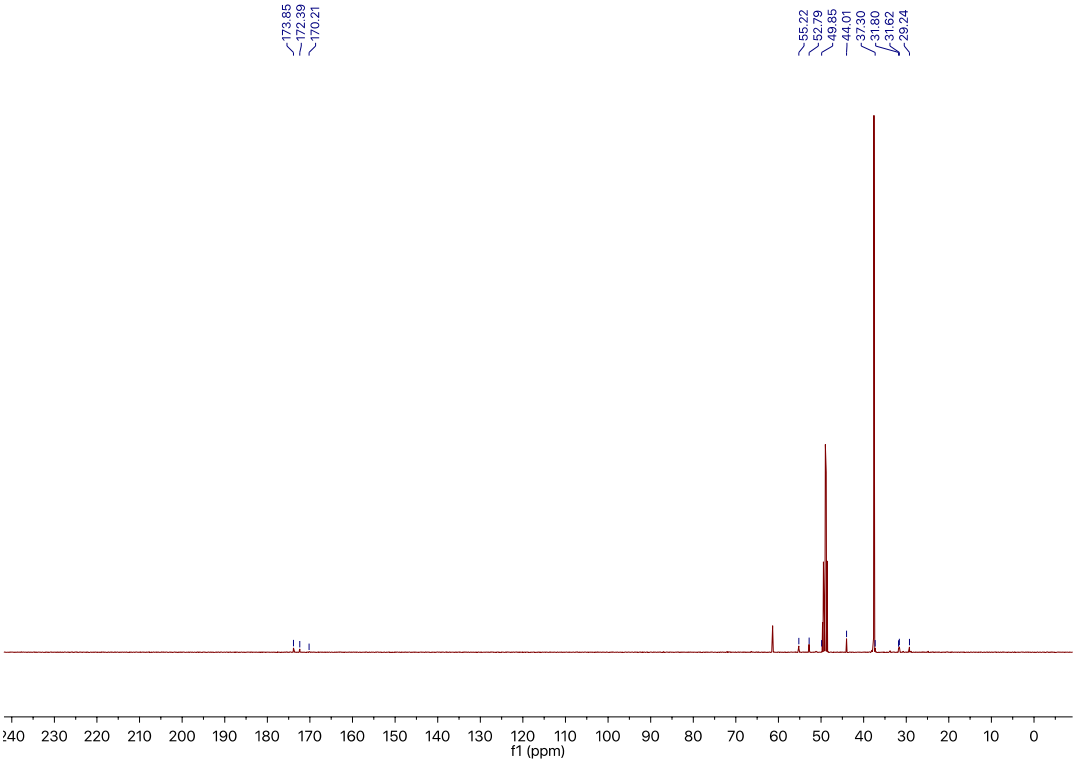

{[(3S)-4-Methoxy-3-(3-{methyl[(13C)methyl]amino}propanamido)-4-oxobutyl]sulfanyl}acetic acid (6**)

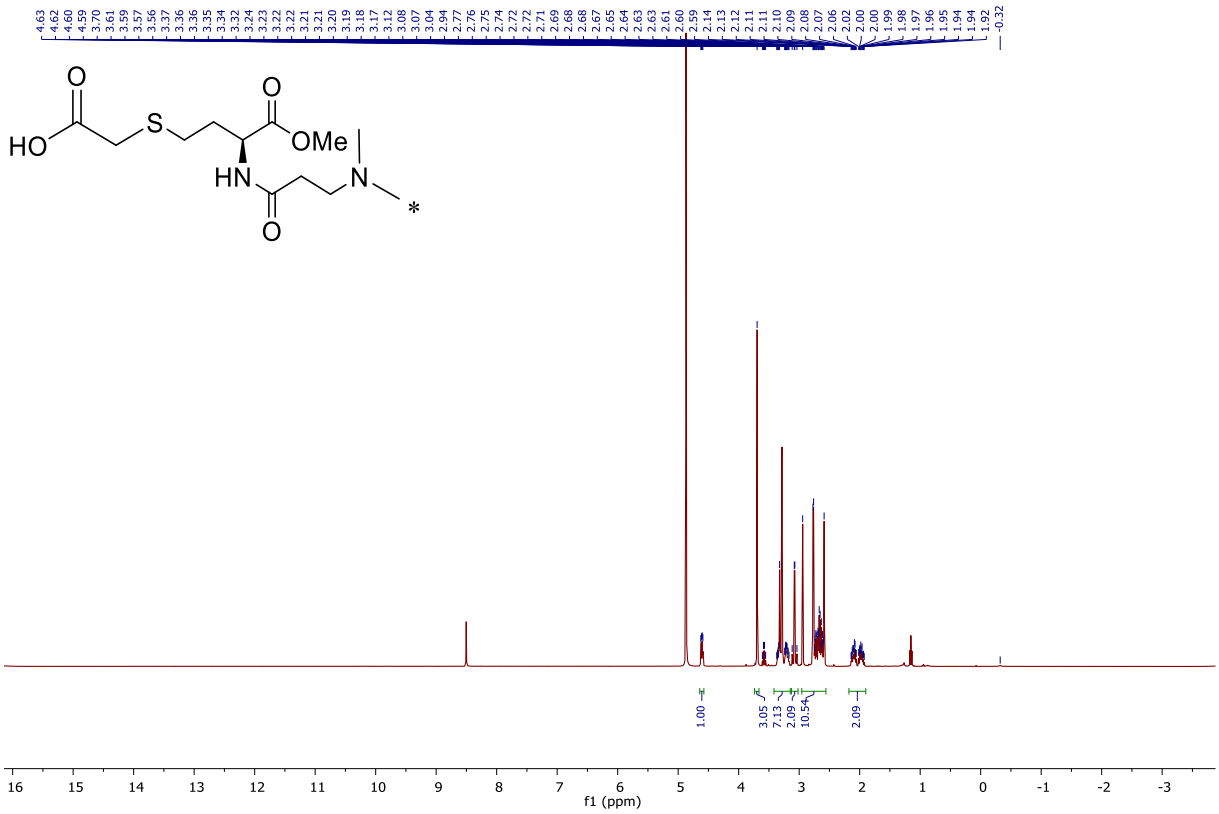

Methyl (2*S*)-4-[(2-{[2-(dimethylamino)ethyl]amino}-2-oxoethyl)sulfanyl]-2-[3-(dimethylamino)propanamido]butanoate (7)

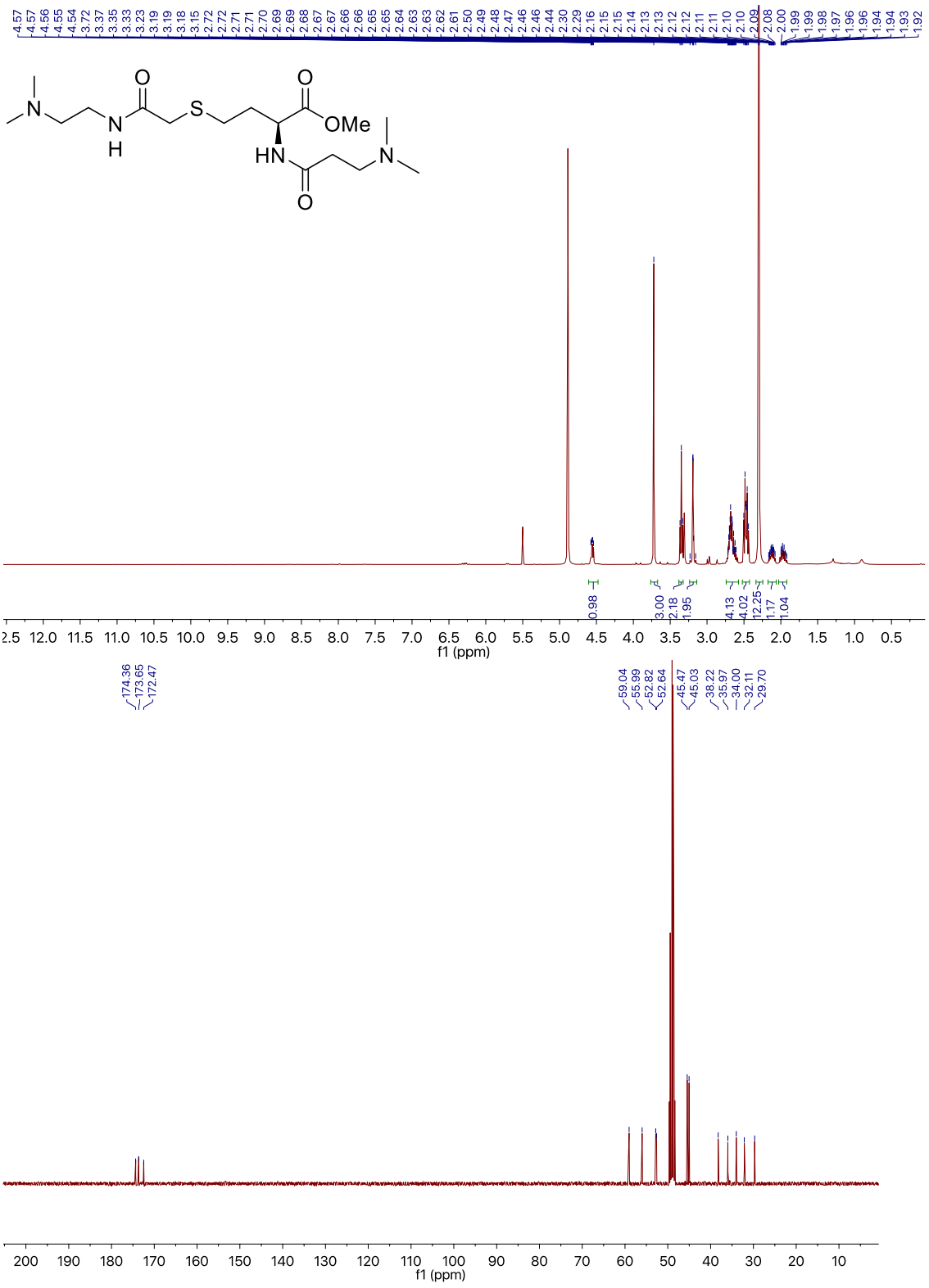

Methyl (2*S*)-4-{[2-{[2-(dimethylamino)ethyl]amino}-2-oxo(1-^{13}C)ethyl]sulfanyl}-2-[3-(dimethylamino)propanamido]butanoate (7*)

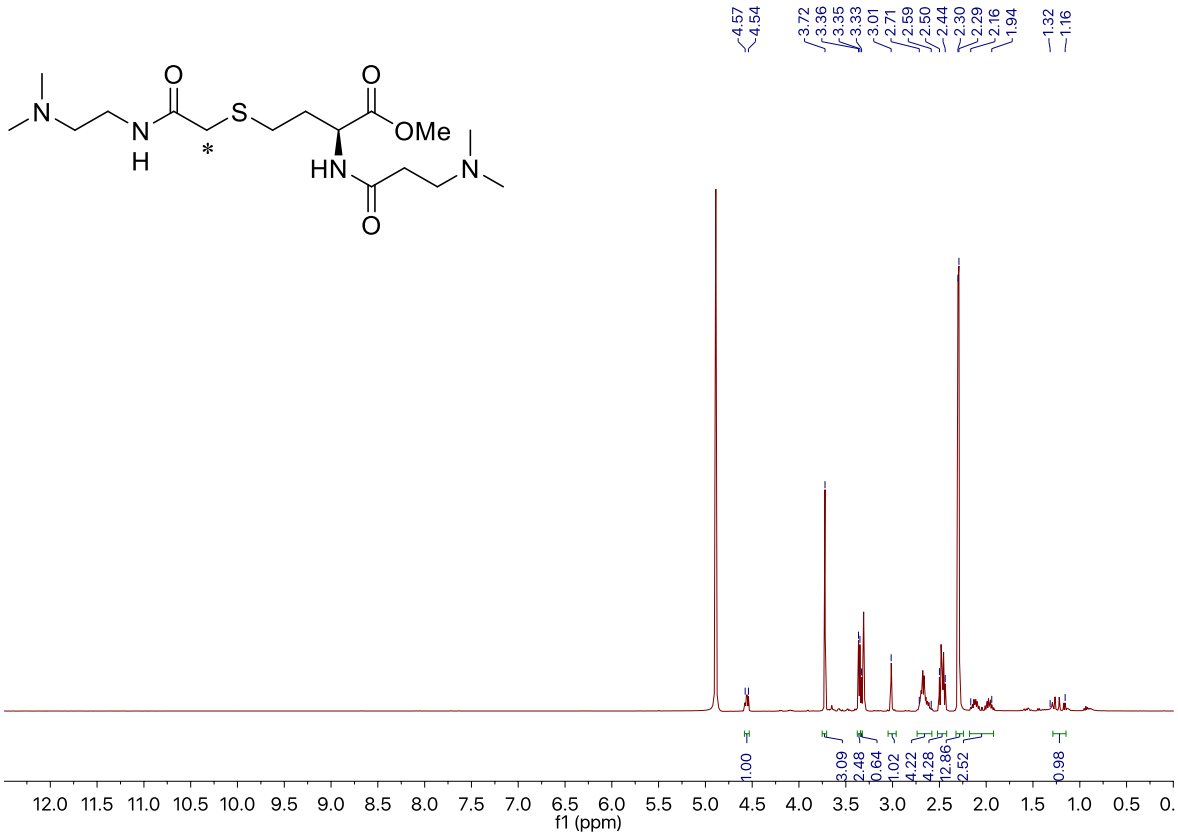

Methyl (2*S*)-4-[(2-{[2-(dimethylamino)ethyl]amino}-2-oxoethyl)sulfanyl]-2-(3-{methyl[(^{13}C)methyl]amino}propanamido)butanoate (7)**

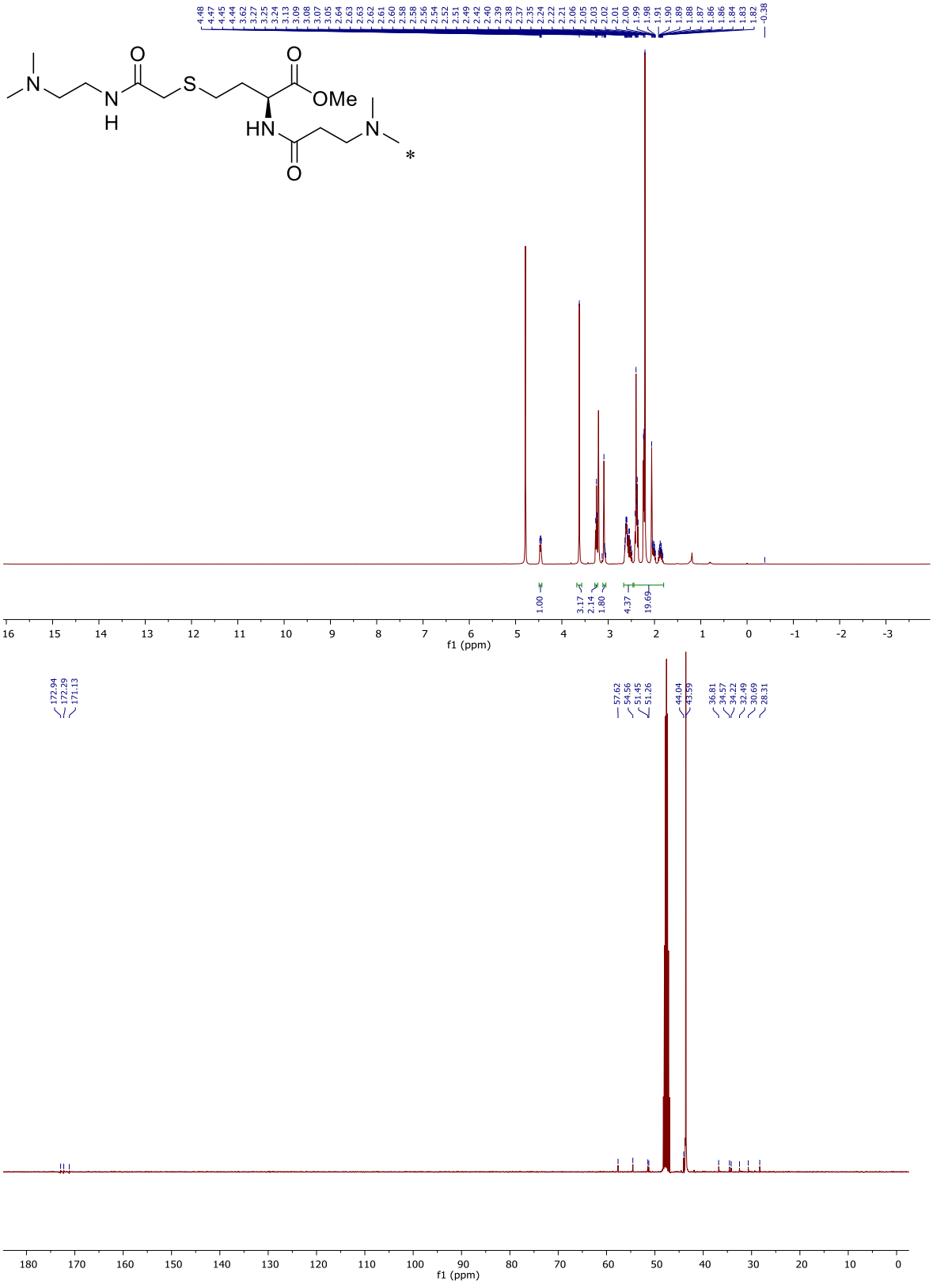

(2*S*)-4-[(2-{[2-(Dimethylamino)ethyl]amino}-2-oxoethyl)sulfanyl]-2-[3-(dimethylamino)propanamido]butanoic acid (8)

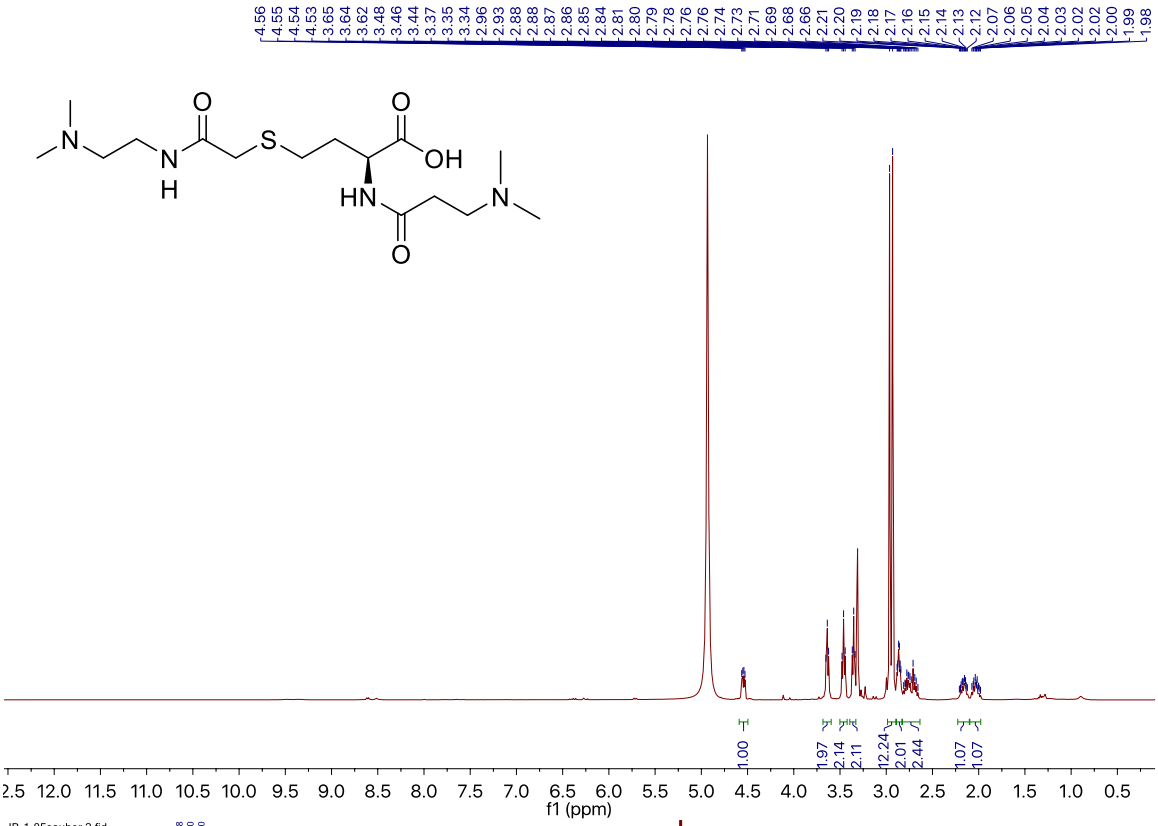

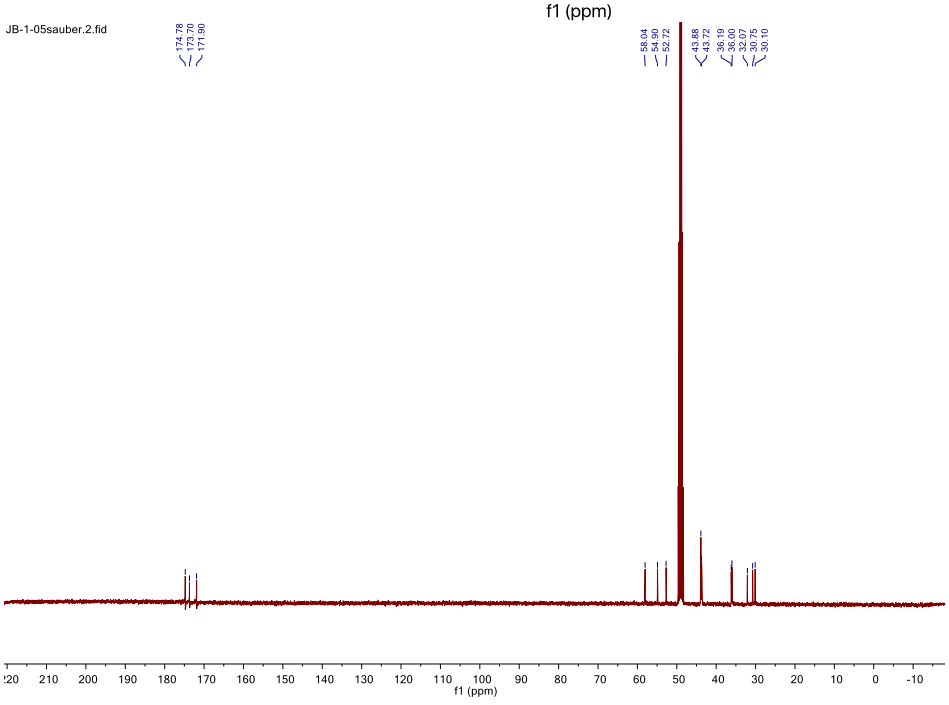

(2*S*)-4-{[2-{[2-(Dimethylamino)ethyl]amino}-2-oxo(1-^{13}C)ethyl]sulfanyl}-2-[3-(dimethylamino)propanamido]butanoic acid (8*)

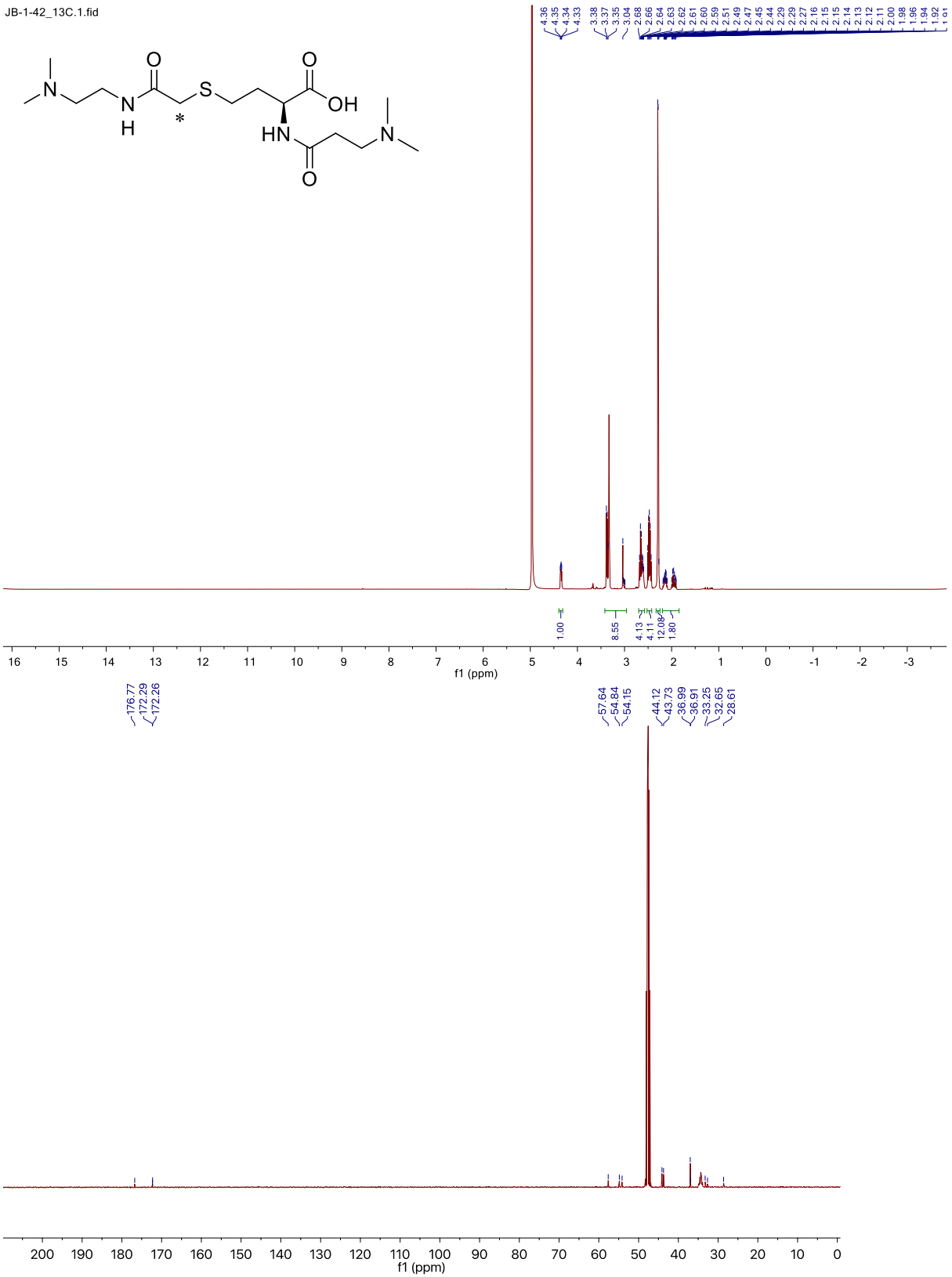

(2*S*)-4-[(2-{[2-(Dimethylamino)ethyl]amino}-2-oxoethyl)sulfanyl]-2-(3-{methyl[(^{13}C)methyl]amino}propanamido)butanoic acid (8)**

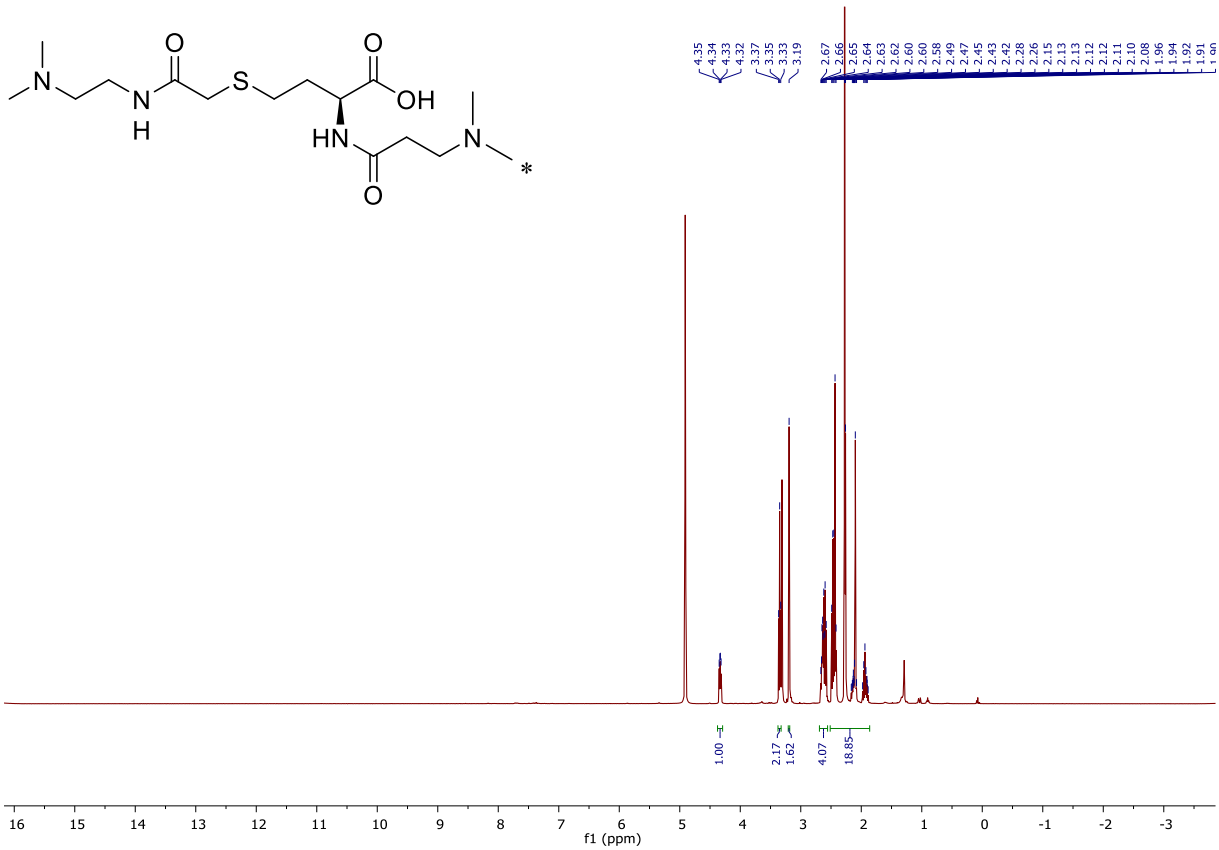

(2*S*)-4-(2-{[2-(Dimethylamino)ethyl]amino}-2-oxoethanesulfinyl)-2-[3-(dimethylamino)propanamido]-butanoic acid (9)

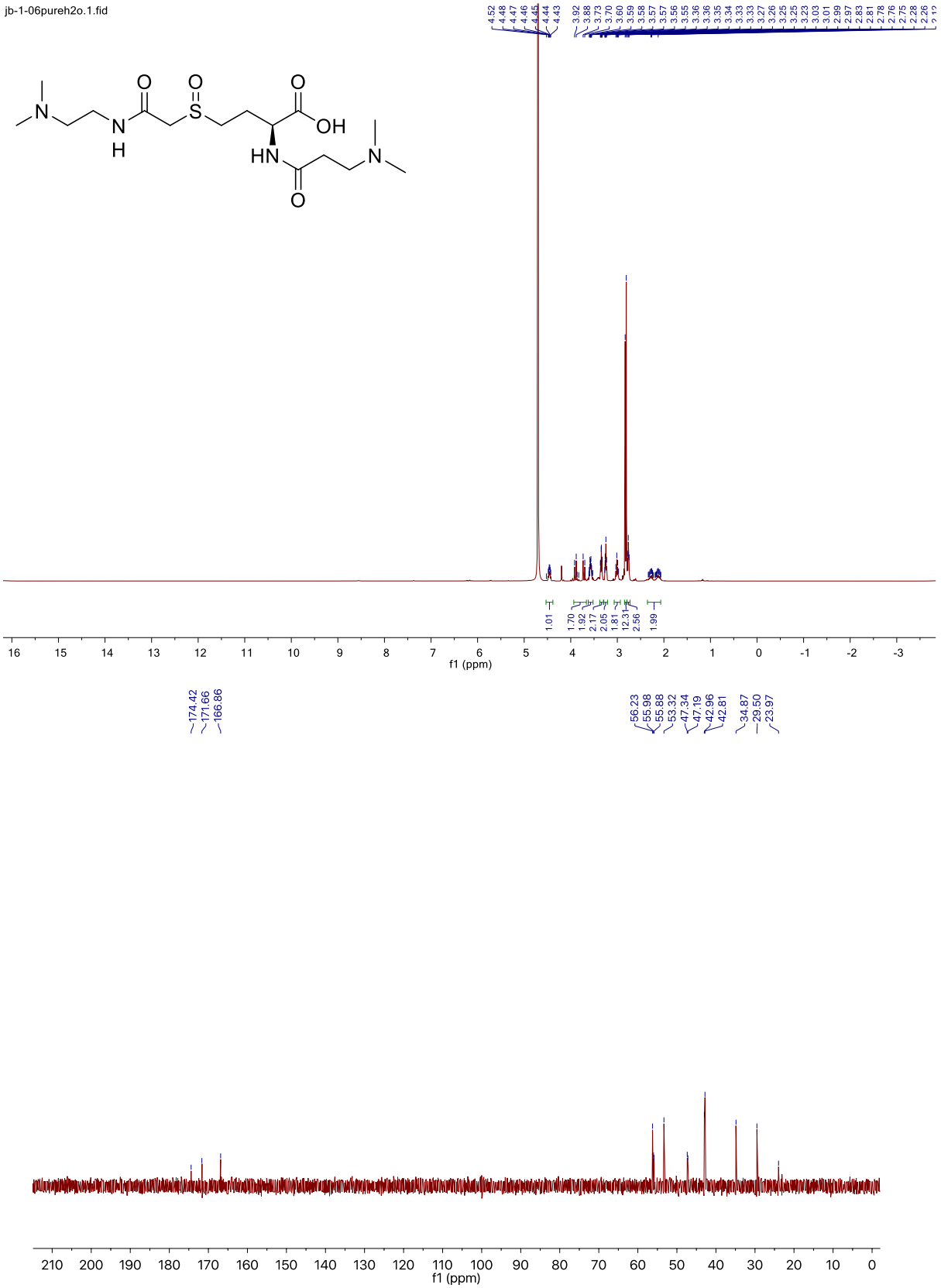

(2*S*)-4-[2-{[2-(Dimethylamino)ethyl]amino}-2-oxo(1-^{13}C)ethanesulfinyl]-2-[3-(dimethylamino)propanamido]-butanoic acid (9*)

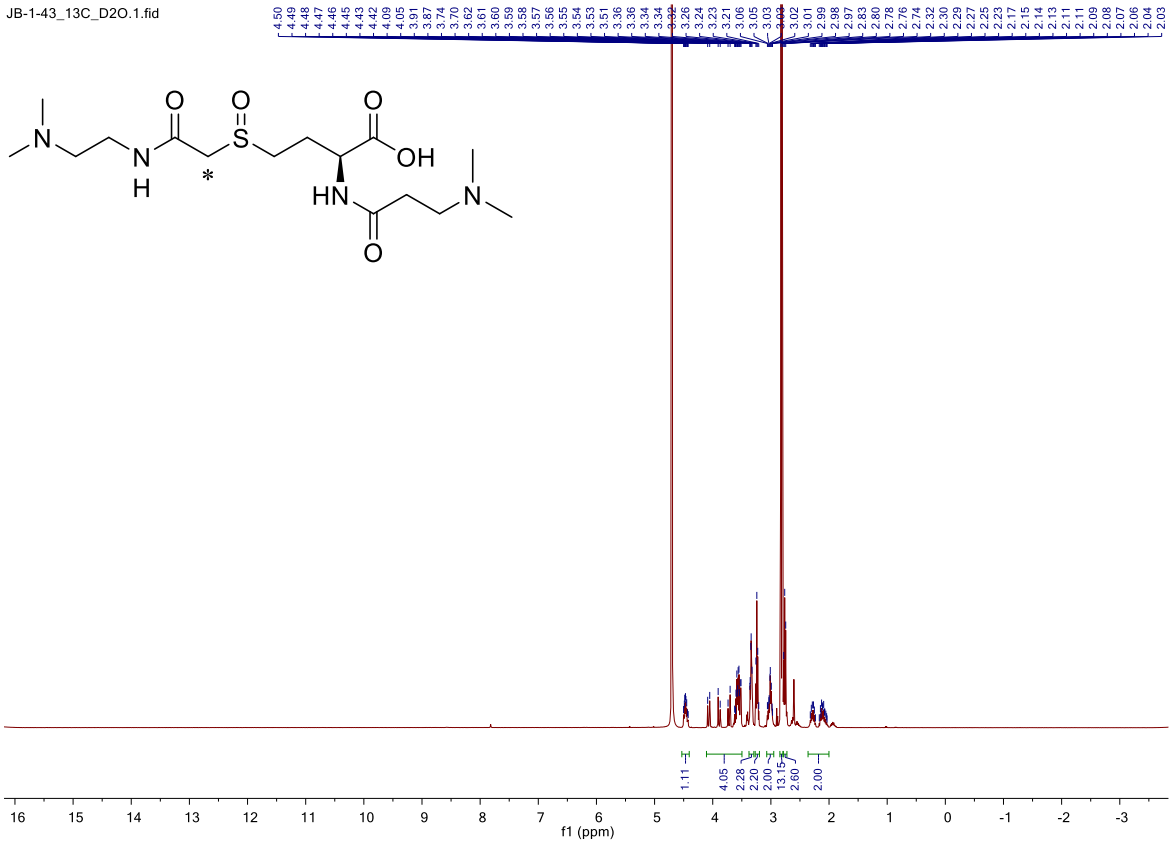

(2*S*)-4-(2-{[2-(Dimethylamino)ethyl]amino}-2-oxoethanesulfinyl)-2-(3-{methyl[(^{13}C)methyl]amino}propanamido)butanoic acid (9)**

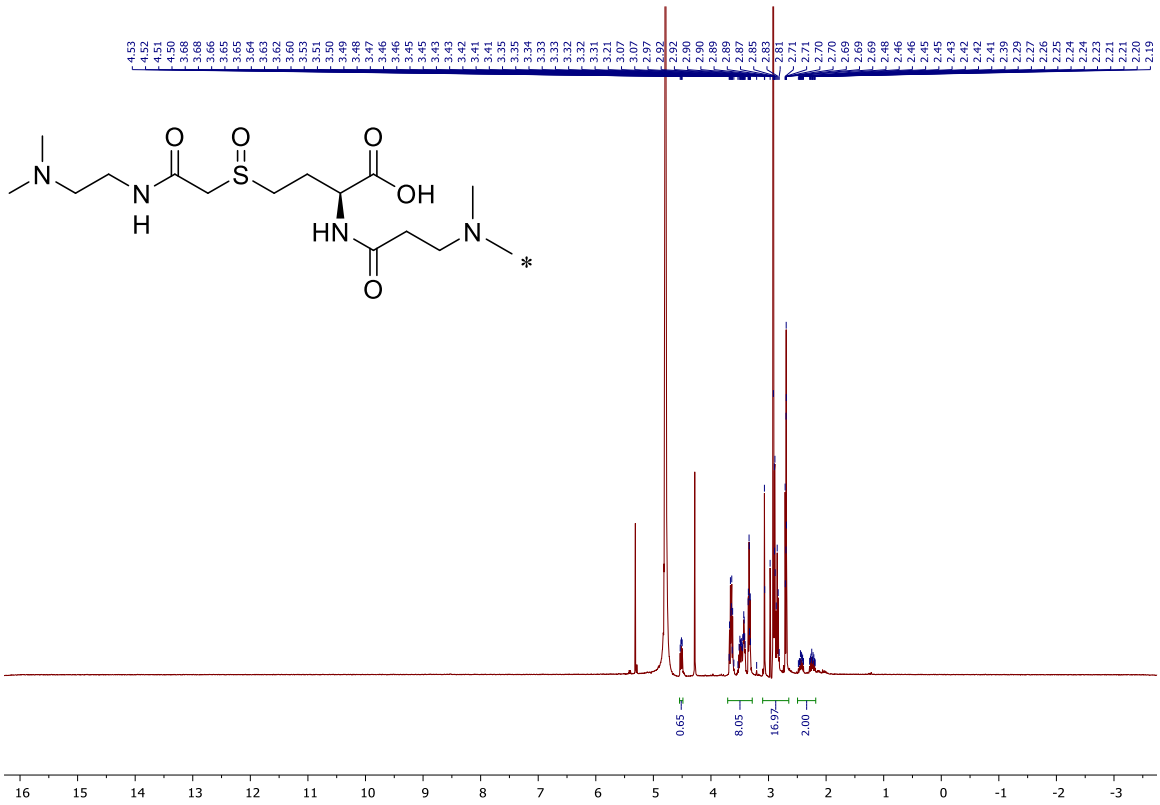

[1] R. Torres Martin de Rosales, R. Tavaré, R. L. Paul, M. Jauregui-Osoro, A. Protti, A. Glaria, G. Varma, I. Szanda, P. J. Blower, *Angew. Chem. International Edition* **2011**, *50*, 5509-5513.

[2] A. J. McShane, Y. Shen, M. J. Castillo, X. Yao, *J. Am. Soc. Mass Spectr.* **2014**, *25*, 1694-1704.

[3] W. Eschweiler, *Ber. Dtsch. Chem. Ges.* **1905**, *38*, 880-882.

[4] H. T. Clarke, H. B. Gillespie, S. Z. Weisshaus, *J. Am. Chem. Soc.* **1933**, *55*, 4571-4587.

[5] N. A. Kulak, G. Pichler, I. Paron, N. Nagaraj, M. Mann, *Nat. Methods* **2014**, *11*, 319-324.

[6] J. Cox, M. Mann, *Nat. Biotechnol.* **2008**, *26*, 1367-1372.

[7] J. Griss, F. Reisinger, H. Hermjakob, J. A. Vizcaíno, *Proteomics* **2012**, *12*, 795-798.

[8] J. Meija, B. Coplen Tyler, M. Berglund, A. Brand Willi, P. De Bièvre, M. Gröning, E. Holden Norman, J. Irrgeher, D. Loss Robert, T. Walczyk, T. Prohaska, *Pure Appl. Chem.* **2016**, *88*, 265.